STRESSES AROUND NEIGHBOURING ELLIPTICAL HOLES IN FLAT PLATES

by

ALKIBIADES ALEXANDRAKIS

S.B., University of Newcastle Upon Tyne

1975

SUBMITTED IN PARTIAL FULFILLMENT

OF THE REQUIREMENTS FOR THE

DEGREE OF MASTER OF

SCIENCE

1976

Signature of Author ....
Department of Ocean Engineering

Certified by ....
Thesis Supervisor

Accepted by ....
Chairman Departmental
(or Interdepartmental Committee)

STRESSES AROUND NEIGHBOURING

ELLIPTICAL HOLES IN FLAT PLATES

by

ALKIBIADES ALEXANDRAKIS

ABSTRACT

The object of this thesis is to examine the application of the overdetermined collocation method to a plane stress problem. After the appropriate series was determined, a computer program was developed which, using the dimensions of the plate, holes and nature of the loading condition and the material as input, would print out stress concentrations as output.

A series of results, testing the numerical method, were obtained and the accuracy observed was found to be acceptable.

Thesis Supervisor: Norman Jones

Title: Professor of Naval Architecture

SECTION I

I. INTRODUCTION

The determination of the stress concentration factors in thin flat elastic plates subjected to in-plane loading and perforated with elliptical or circular holes has been a problem widely studied, either theoretically or experimentally, for a long time.

However, the particular case of the interaction stresses around neighboring elliptical holes has not attracted as much attention and the references on the subject are surprisingly few. Goldberg and Jabbour [5] have considered plates perforated with hexagonal arrays of circular holes while Slot and Yalch [1] have analysed the cases of plates perforated with a triangular hole pattern subjected to a uniform normal stress along the edge and have developed a suitable computer program.

Virtually all of the experimental results in this field have been obtained by the method of photoelasticity ([2] and [9]).

The problem under consideration could be easily approached by already existing finite element procedures but the purpose of this study was to provide a more theoretical approach by making use of an overdetermined collocation method developed in [4] and used in [2] subject to the comments and recommended refinements in [7]. Thus the use of an expensive finite element computing technique was avoided.

A computer program was developed, as described in Section III of this thesis, that will print out the stresses at selected points on the elliptical boundary, after requiring an input consisting of the dimensions of the plate and the elliptical hole, the loading conditions and the separation of the two holes.

The results thus obtained were compared against those presented in [2] for the case of neighboring elliptical holes having parallel minor axes.

SECTION II

THEORETICAL DEVELOPMENT

II.1. DEFINITION OF GENERAL PROBLEM

The most general form of the problem is the following: A thin flat plate of length W_x and breadth W_y, perforated with one or more elliptical holes of major axis 2a and minor axis 2b is subjected to a biaxial load, σ_1 parallel to W_x and σ_2 parallel to W_y. Of course, σ_2 and σ_2 can be either positive or negative, i.e., either tensile or compressive loads.

The first observation to be made is that there are two types of boundaries in the case under consideration, namely rectangular and elliptical. So the nature of the problem suggests the use of an elliptical coordinate system provided of course that proper relations will exist for transferring control from the elliptical to the Cartesian coordinates when considering stresses and deflections along the plate edges.

The second important point is that elasticity is assumed for all loading conditions to be considered so that perfect stress-strain relationships will be true throughout.

Finally, the following assumptions must be valid for the theory subsequently described to be true:

1. Isotropic elastic material
2. Thin flat plate
3. Two-dimensional stress system

II.2. GENERAL OUTLINE OF THEORETICAL DEVELOPMENT

This chapter contains the general theoretical basis of the problem as developed by Professor N. Jones. A brief outline of this theory is also contained in [2].

The basic equations of transformation from Cartesian to elliptical coordinates are

$$x = c \cosh\xi \; \cos\eta \tag{1}$$

$$y = c \sinh\xi \; \sin\eta \tag{2}$$

By imposing the condition η=constant to the above, a family of confocal hyperbolae is obtained, the equation of which is

$$\frac{x^2}{c^2\cos^2\eta} - \frac{y^2}{c^2\sin^2\eta} = 1 \tag{3}$$

In a similar way, the condition ξ=constant, yields a family of confocal ellipses whose equation is

$$\frac{x^2}{c^2\cosh^2\xi} + \frac{y^2}{c^2\sinh^2\xi} = 1 \tag{4}$$

The elliptical coordinates of a point (x,y) are shown in Fig. 2.

It can be easily shown that (1) and (2) satisfy a set of Cauchy Rieman conditions

$$\left(\frac{\partial x}{\partial \xi}\right)_\eta = \left(\frac{\partial y}{\partial \eta}\right)_\xi$$

$$\left(\frac{\partial x}{\partial \eta}\right)_\xi = - \frac{\partial y}{\partial \xi}\Big)_\eta \tag{5}$$

Furthermore, it is true that

$$\left(\frac{\partial^2 x}{\partial \xi^2}\right)_\eta = -\left(\frac{\partial^2 x}{\partial \eta^2}\right)_\xi$$

$$\left(\frac{\partial^2 y}{\partial \xi^2}\right)_\eta = -\left(\frac{\partial^2 y}{\partial \eta^2}\right)_\xi \qquad (6)$$

Also (3) and (4) yield the following results

$$\left(\frac{\partial \xi}{\partial x}\right)_y = \left(\frac{\partial \eta}{\partial y}\right)_x$$

$$\left(\frac{\partial \xi}{\partial y}\right)_x = -\left(\frac{\partial \eta}{\partial x}\right)_y \qquad (7)$$

and

$$\left(\frac{\partial^2 \xi}{\partial x^2}\right)_y = -\left(\frac{\partial^2 \xi}{\partial y^2}\right)_x$$

$$\left(\frac{\partial^2 \eta}{\partial x^2}\right)_y = -\left(\frac{\partial^2 \eta}{\partial y^2}\right)_x \qquad (8)$$

Now, if a general function $\psi(x,y)$ is transformed to $\phi(\xi,\eta)$, the following relations are true

$$\frac{\partial \psi}{\partial x} = \frac{\partial \phi}{\partial \xi}\frac{\partial \xi}{\partial x} + \frac{\partial \phi}{\partial \eta}\frac{\partial \eta}{\partial x} \qquad (9a)$$

$$\frac{\partial \psi}{\partial y} = \frac{\partial \phi}{\partial \xi}\frac{\partial \xi}{\partial y} + \frac{\partial \phi}{\partial n}\frac{\partial \eta}{\partial y} \qquad (9b)$$

and also

$$\frac{\partial^2 \psi}{\partial x^2} = \frac{\partial^2 \phi}{\partial \xi^2}\left(\frac{\partial \xi}{\partial x}\right)^2 + \frac{\partial^2 \phi}{\partial \eta^2}\left(\frac{\partial \eta}{\partial x}\right)^2 + 2\frac{\partial^2 \phi}{\partial \xi \partial \eta}\left(\frac{\partial \xi}{\partial x}\right)\left(\frac{\partial \eta}{\partial x}\right) +$$

$$\frac{\partial \phi}{\partial \xi}\frac{\partial^2 \xi}{\partial x^2} + \frac{\partial \phi}{\partial \eta}\frac{\partial^2 \eta}{\partial x^2} \qquad (10)$$

$$\frac{\partial^2\psi}{\partial y^2} + \frac{\partial^2\phi}{\partial\xi^2}\left(\frac{\partial\xi}{\partial y}\right)^2 + \frac{\partial^2\phi}{\partial\eta^2}\left(\frac{\partial\eta}{\partial y}\right)^2 + 2\,\frac{\partial^2\phi}{\partial\eta\partial\xi}\left(\frac{\partial\xi}{\partial y}\right)\left(\frac{\partial\eta}{\partial y}\right) +$$

$$\frac{\partial\phi}{\partial\eta}\frac{\partial^2\eta}{\partial y^2} + \frac{\partial\phi}{\partial\xi}\frac{\partial^2\xi}{\partial y^2} \qquad (11)$$

as well as

$$\frac{\partial^2\psi}{\partial x\partial y} = \frac{\partial^2\psi}{\partial y\partial x} = \frac{\partial^2\phi}{\partial\xi^2}\frac{\partial\xi}{\partial x}\frac{\partial\xi}{\partial y} + \frac{\partial^2\phi}{\partial\xi\partial\eta}\frac{\partial\eta}{\partial x}\frac{\partial\xi}{\partial y} + \frac{\partial\phi}{\partial\xi}\frac{\partial^2\xi}{\partial y\partial x} +$$

$$\frac{\partial^2\phi}{\partial\eta\partial\xi}\frac{\partial\xi}{\partial x}\frac{\partial\eta}{\partial y} + \frac{\partial^2\phi}{\partial\eta^2}\frac{\partial\eta}{\partial x}\frac{\partial\eta}{\partial y} + \frac{\partial\phi}{\partial\eta}\frac{\partial^2\eta}{\partial y\partial x} \qquad (12)$$

Now, if the function Φ is selected in such a way that

$$\sigma_x = \frac{\partial^2\phi}{\partial y^2}\,;\quad \sigma_y = \frac{\partial^2\phi}{\partial x^2}\,;\quad \tau_{xy} = -\frac{\partial^2\phi}{\partial x\partial y} \qquad (13)$$

it can be easily shown from general stress considerations in a two-dimensional stress system that these satisfy the biharmonic equation

$$\nabla^4\phi = 0 \qquad (14)$$

or, more explicitly

$$\frac{\partial^4\phi}{\partial x^4} + 2\,\frac{\partial^4\phi}{\partial x^2\partial y^2} + \frac{\partial^4\phi}{\partial y^4} = 0 \qquad (14a)$$

Now, from Fig. 2, using (1) and (2)

$$\text{Slope} = \left(\frac{dy}{dx}\right) = \frac{(\partial y/\partial\eta)\xi}{(\partial x/\partial\eta)_\xi} = -\tanh\xi\,\cot\eta$$

So, by trigonometric manipulation,

$$\sin\,\alpha - \frac{\sinh\xi\ \cos\eta}{\sqrt{\sin^2\eta + \sinh^2\xi}}$$

$$\cos\,\alpha - \frac{\sin\eta\ \cosh\xi}{\sqrt{\sin^2\eta+\sinh^2\xi}} \qquad (15)$$

Using Fig. 3, and resolving stress components, we obtain

$$\sigma_x = \sigma_\xi\ \sin^2\alpha + \sigma_\eta\ \cos^2\alpha = \tau_{\xi\eta}\ \sin 2\alpha \qquad (16)$$

Similarly, expressions for σ_y and τ_{xy} are obtained and thus

$$\sigma_y = \sigma_\xi\ \cos^2\alpha + \sigma_\eta\ \sin^2\alpha + \tau_{\xi\eta}\ \sin\,2\alpha \qquad (17)$$

$$\tau_{xy} - \frac{1}{2}\,(\sigma_\xi - \sigma_\eta)\ \sin 2\alpha - \tau_{\xi\eta}\cos 2\alpha \qquad (18)$$

Solving (16), (17) and (18) for the stresses in elliptical coordinates, i.e., $(\sigma_\xi,\ \sigma_\eta,\ \tau_{\xi\eta})$

$$\sigma_\xi = \sigma_x\sin^2\alpha + \sigma_y\cos^2\alpha - \tau_{xy}\sin 2\alpha \qquad (19)$$

$$\sigma_\eta = \sigma_x\cos^2\alpha + \sigma_y\sin 2\alpha - \tau_{xy}\sin 2\alpha \qquad (20)$$

$$\tau_{\xi\eta} = \frac{1}{2}\,(\sigma_x - \sigma_y)\sin 2\alpha + \tau_{xy}\cos 2\alpha \qquad (21)$$

Using (19), (20), (21) and employing (15) as well as (5) through (12), the following expressions for the stresses in elliptical coordinates are obtained

$$J^2\sigma_\xi = \frac{\partial^2\phi}{\partial\eta^2} - \frac{c^2\sin\eta\cos\eta}{J^2}\frac{\partial\phi}{\partial\eta} + \frac{c^2\sinh\xi\cosh\xi}{J^2}\frac{\partial\phi}{\partial\xi} \tag{22}$$

$$J^2\sigma\eta = \frac{\partial^2\phi}{\partial\xi^2} - \frac{c^2\sinh\xi\cosh\xi}{J^2}\frac{\partial\phi}{\partial\xi} + \frac{c^2\sin\eta\cos\eta}{J^2}\frac{\partial\phi}{\partial\eta} \tag{23}$$

$$J^2\tau_{\xi\eta} = -\frac{\partial^2\phi}{\partial\eta\partial\xi} + \frac{c^2\sin\eta\cos\eta}{J^2}\frac{\partial\phi}{\partial\xi} + \frac{c^2\sinh\xi\cosh\xi}{J^2}\frac{\partial\phi}{\partial\eta} \tag{24}$$

where

$$J^2 - \frac{c^2}{2}(\cosh 2\xi - \cos 2\eta) \tag{25}$$

Now, the following functions can be seen to satisfy the biharmonic equation (14)

$$\psi_1 = e^{(n+1)\xi}\cos[(n-1)\eta] + e^{(n-1)\xi}\cos[(n+1)\eta] \tag{26a}$$

$$\psi_2 = e^{-(n+1)\xi}\cos[(n-1)\eta] + e^{-(n-1)\xi}\cos[(n+1)\eta] \tag{26b}$$

$$\psi_3 = e^{(n+1)\xi}\sin[(n-1)\eta] + e^{(n-1)\xi}\sin[(n+1)\eta] \tag{26c}$$

$$\psi_4 = e^{-(n+1)\xi}\sin[(n-1)\eta] + e^{-(n-1)\xi}\sin[(n+1)\eta] \tag{26d}$$

$$\psi_5 = e^{n\xi}\cos n\eta \tag{26e}$$

$$\psi_6 = e^{-n\xi}\cos n\eta \tag{26f}$$

$$\psi_7 = e^{n\xi}\sin n\eta \tag{26g}$$

$$\psi_8 = e^{-n\xi}\sin n\eta \tag{26h}$$

$$\psi_9 = \xi \tag{26i}$$

$$\psi_{10} = \eta \tag{26j}$$

Therefore, a linear combination of all the above is possible that would satisfy (14). In this way the general stress function Φ is obtained as follows

$$\begin{aligned}
\Phi = a_o\xi + b_o\eta + \sum_{n=0}^{\infty} & c_n[e^{(n+1)\xi}\cos(n-1)\eta + e^{(n-1)\xi}\cos(n+1)\eta\ ] + \\
& d_n[e^{-(n+1)\xi}\cos(n-1)\eta + e^{-(n-1)\xi}\cos(n+1)\eta] + \\
& e_n[e^{(n+1)\xi}\sin(n-1)\eta + e^{(n-1)\xi}\sin(n+1)\eta] + \\
& f_n[e^{-(n-1)\xi}\sin(n-1)\eta + e^{-(n-1)\xi}\sin(n+1)\eta] + \\
& g_n[e^{n\xi}\cos n\eta] + \\
& h_n[e^{-n\xi}\cos n\eta] + \\
& j_n[e^{n\xi}\sin n\eta] + \\
& k_n[e^{-n\xi}\sin n\eta]
\end{aligned} \tag{27}$$

Using (27) we can substitute into (22), (23), (24) to obtain general expressions for the stresses in elliptical coordinates in the following way

$$c^2\ (\cosh 2\xi\ -\ \cos 2\eta)^2\sigma_\xi\ =$$

$$\sum_{n=0}^{\infty} n\ \cos(n+3)\eta[c_n(n+1)e^{(n-1)\xi}+d_n(n+1)e^{-(n-1)\xi}]\ +$$

$$\cos(n+1)\eta[-4c_n e^{(n+1)\xi}\ -\ c_n(n+3)e^{(n-3)\xi}\ -\ 4d_n e^{-(n+1)\xi}$$

$$-d_n(n+3)e^{-(n-3)\xi}]\ +$$

$$\cos(n-1)\eta[4c_n e^{(n-1)\xi}\ -\ c_n(n-3)e^{(n+3)\xi}\ +\ 4d_n e^{-(n-1)\xi}$$

$$-d_n(n-3)e^{-(n+3)\xi}]\ +$$

$$\cos(n-3)\eta[c_n(n-1)e^{(n+1)\xi}\ +\ d_n(n-1)e^{-(n+1)\xi}]\ +$$

$$\sin(n+2)\eta[j_n(n-1)e^{n\xi}\ +\ k_n(n-1)e^{-n\xi}]\ +$$

$$\sin n\eta[-j_n(n-1)e^{(n+3)\xi}\ -\ j_n(n+1)e^{(n-2)\xi}\ -\ k_n(n-1)e^{-(n+2)\xi}$$

$$-k_n(n+1)e^{-(n-2)\xi}]\ +$$

$$\sin(n-2)\eta[j_n(n+1)e^{n\xi}\ +\ k_n(n+1)e^{-n\xi}]\ +$$

$$\cos(n+2)\eta[g_n(n-1)e^{n\xi}\ +\ h_n(n-1)e^{-n\xi}]\ +$$

$$\cos n\eta[-g_n(n-1)e^{(n+2)\xi}\ -\ g_n(n+1)e^{(n-2)\xi}\ -\ h_n(n-1)e^{-(n+2)\xi}$$

$$-h_n(n+1)e^{-(n-2)\xi}]\ +$$

$$\cos(n-2)\eta[g_n(n+1)e^{n\xi}\ +\ h_n(n+1)e^{-n\xi}]\ +$$

$$\sin(n+3)\eta[e_n(n+1)e^{(n-1)\xi} + f_n(n+1)e^{-(n-1)\xi}] \ +$$

$$\sin(n+1)\eta[-4e_n e^{(n+1)\xi} - e_n(n+3)e^{(n-3)\xi} - 4f_n e^{-(n+1)\xi}$$

$$-f_n(n+3)e^{-(n-3)\xi}] \ +$$

$$\sin(n-1)\eta[4e_n e^{(n-1)\xi} - e_n(n-3)e^{(n+3)\xi} + 4f_n e^{-(n-1)\xi}$$

$$-f_n(n-3)e^{-(n+3)\xi}] \ +$$

$$\sin(n-3)\eta[e_n(n-1)e^{(n+1)\xi} + f_n(n-1)e^{-(n+1)\xi}] \ +$$

$$2a_o \sinh 2\xi \ +$$

$$2b_o \sin 2\eta \tag{28}$$

Similarly,

$$c^2(\cosh 2\xi - \cos 2\eta)^2 \sigma_\eta =$$

$$\sum_{n=0}^{\infty} n \cos(n+3)\eta[-c_n(n-3)e^{(n-1)\xi} - d_n(n-3)e^{-(n-1)\xi}] \ +$$

$$\cos(n+1)\eta[-c_n 4e^{(n+1)\xi} + c_n(n-1)e^{(n-3)\xi} - d_n 4e^{-(n+1)\xi}$$

$$+d_n(n-1)e^{-(n-3)\xi}] \ +$$

$$\cos(n-1)\eta[c_n 4e^{(n-1)\xi} + c_n(n+1)e^{(n+3)\xi} + d_n 4e^{-(n-1)\xi}$$

$$+d_n(n+1)e^{-(n+3)\xi}] \ +$$

$$\cos(n-3)\eta[-c_n(n+3)e^{(n+1)\xi} - d_n(n+3)e^{-(n+1)\xi}] \ +$$

$$\sin(n+2)\eta[-j_n(n-1)e^{n\xi} - k_n(n-1)e^{-n\xi}] \ +$$

$$\sin n\eta\,[j_n(n-1)e^{(n+2)\xi} + j_n(n+1)e^{(n-2)\xi} + k_n(n-1)e^{-(n+2)\xi} +$$

$$k_n(n+1)e^{-(n-2)\xi}] \quad +$$

$$\sin(n-2)\eta\,[-j_n(n+1)e^{n\xi} - k_n(n+1)e^{-n\xi}] +$$

$$\cos(n+2)\eta\,[-g_n(n-1)e^{n\xi} - h_n(n-1)e^{-n\xi}] +$$

$$\cos n\eta\,[g_n(n-1)e^{(n+2)\xi} + g_n(n+1)e^{(n-2)\xi} + h_n(n-1)e^{-(n+2)\xi} +$$

$$h_n(n+1)e^{-(n-2)\xi}] \quad +$$

$$\cos(n-2)\eta\,[-g_n(n+1)e^{n\xi} - h_n(n+1)e^{-n\xi}] \quad +$$

$$\sin(n+3)\eta\,]-e_n(n-3)e^{(n-1)\xi} - f_n(n-3)e^{-(n-1)\xi}] +$$

$$\sin(n+1)\eta\,[-e_n 4e^{(n+1)\xi} + e_n(n-1)e^{(n-3)\xi} - f_n 4e^{-(n+1)\xi} +$$

$$f_n(n-1)e^{-(n-3)\xi}] \quad +$$

$$\sin(n-1)\eta\,[e_n 4e^{(n-1)\xi} + e_n(n+1)e^{(n+3)\xi} + f_n 4e^{-(n-1)\xi} +$$

$$f_n(n+1)e^{-(n+3)\xi}] \quad +$$

$$\sin(n-3)\eta\,[-e_n(n+3)e^{(n+1)\xi} - f_n(n+3)e^{-(n+1)\xi}] \quad -$$

$$2a_o \sinh 2\xi \quad +$$

$$2b_o \sin 2\eta \qquad (29)$$

and finally

$$c^2(\cosh 2\xi \; - \cos^2\eta)^2\tau_{\xi\eta} \; =$$

$$\sum_{n=0}^{\infty} n \quad \sin(n+3)\eta[-c_n(n-1)e^{(n-1)\xi} + d_n(n-1)e^{-(n-1)\xi} +$$

$$\sin(n+1)\eta[c_n(n+1)e^{(n-3)\xi} - d_n(n+1)e^{-(n-3)\xi}] +$$

$$\sin(n-1)\eta[c_n(n-1)e^{(n+3)\xi} - d_n(n-1)e^{-(n+3)\xi}] +$$

$$\sin(n-3)\eta[-c_n(n-1)e^{(n+1)\xi} + d_n(n=1)e^{-(n+1)\xi}] +$$

$$\cos(n+2)\eta[j_n(n-1)e^{n\xi} - k_n(n-1)e^{-n\xi} \;] \; +$$

$$\cos n\eta[-j_n(n-1)e^{(n+2)\xi} - j_n(n+1)e^{(n-2)\xi} + k_n(n-1)e^{-(n+2)\xi}$$

$$+ k_n(n+1)e^{-(n-2)\xi} \;] \; +$$

$$\cos(n-2)\eta[j_n(n+1)e^{n\xi} - k_n(n+1)e^{-n\xi}] \; +$$

$$\sin(n+2)\eta[-g_n(n-1)e^{n\xi} + h_n(n-1)e^{-n\xi}] \; +$$

$$\sin n\eta[g_n(n-1)e^{(n+2)\xi} + g_n(n+1)e^{(n-2)\xi} - h_n(n-1)e^{-(n+2)\xi}$$

$$-h_n(n+1)e^{-(n-2)\xi}] \; +$$

$$\sin(n-2)\eta[g_n(n+1)e^{n\xi} + h_n(n+1)e^{-n\xi}] \; +$$

$$\cos(n+3)\eta[e_n(n-1)e^{(n-1)\xi} - f_n(n-1)e^{-(n-1)\xi}] \; +$$

$$\cos(n+1)\eta[-e_n(n+1)e^{(n-3)\xi} + f_n(n+1)e^{-(n-3)\xi}] \; +$$

$$\cos(n-1)\eta[-e_n(n-1)e^{(n+e)\xi} - f_n(n-1)e^{-(n+3)\xi}] \; +$$

$$\cos(n-3)\eta[e_n(n+1)e^{(n+1)\xi} - f_n(n+1)e^{-(n+1)\xi}] +$$

$$2a_o \sin 2\eta +$$

$$2b_o \sinh 2\xi \qquad (30)$$

For each particular case, the corresponding boundary conditions can be assumed. Then, truncation of (28), (29), (30) will yield a certain number of unknown constants which can be determined by satisfying the boundary conditions at an appropriate number of points and then solving the resulting system of simultaneous equations. Such a procedure will be shown explicitly for the case of a two hole plate.

II.3. DETERMINATION OF THE DISPLACEMENT FUNCTIONS

The previous chapter deals with the development of the general stress equations expressed either in elliptical or cartesian coordinates. However, consideration of the boundary conditions as mentioned towards the end of that chapter, will also present displacement as well as stress equations and, consequently, the general displacement functions must be determined.

(Using [10] the generalized Hookes law can be written as

$$\sigma_{ij} = \lambda\theta + 2\mu e_{ij} \tag{31}$$

where in this case

$$\theta = e_{\xi\xi} + e_{\eta\eta} + e_{jj} \tag{32}$$

and λ and μ are Lomes constants defined as

$$\lambda = \frac{Ev}{(1+r)(1-2r)}$$

$$\mu = \frac{E}{2(1+\nu)} = G \tag{33}$$

Therefore, from (31), due to (32)

$$\sigma_{\xi\xi} = \lambda[e_{\xi\xi} + e_{\eta\eta} + e_{ii}] + 2\mu e_{\xi\xi}$$

$$\sigma_{\xi\xi} = [\lambda(1-\nu)+2\mu]e_{\xi\xi} + \lambda(1-\nu)e_{\eta\eta} \tag{34}$$

using the fact that

$$e_{jj} = -\nu(e_{\xi\xi} + e_{\eta\eta}) \quad \text{for plane stress}$$

or, in simpler notation,

$$\sigma_{\xi} = [\lambda(1-\nu)+2\mu]e_{\xi} + \lambda(1-\nu)e_{\eta} \qquad (34a)$$

Similarly,

$$\sigma_{\eta} = [\lambda(1-\nu) + 2\mu]\, e_{\eta} + \lambda(1-\nu)e_{\xi} \qquad (35)$$

and

$$\tau_{\xi\eta} = \mu e_{\xi\eta} \qquad (36)$$

Now, from [3] the following relations are true between strains and displacements expressed in the (ξ,η) coordinate system

$$e_{\xi} = h[\frac{\partial u_{\xi}}{\partial \xi} + \frac{u_{\eta}\sin 2\eta}{\cosh 2\xi - \cos 2\eta}]$$
$$e_{\eta} = h[\frac{\partial u_{\eta}}{\partial \eta} + \frac{u_{\xi}\sinh 2\xi}{\cosh 2\xi - \cos 2\eta}] \qquad (38)$$

where

$$h = \sqrt{\frac{2}{c^2(\cosh 2\xi - \cos 2\eta)}} \qquad (39)$$

Then, following a procedure similar to that of [3] (but for a two-dimensional <u>stress</u> system instead of a two-dimensional <u>strain</u> system) the following general displacement functions were obtained (see Appendix 4)

$$\frac{u_\xi}{h} = \sum_{n=0}^{\infty} \quad c_n[-A_n e^{(n+1)\xi}\cos(n-1)\eta - B_n e^{(n-1)\xi} \cos(n+1)\eta] \quad +$$

$$d_n[A_n e^{-(n+1)\xi}\cos(n-1)\eta + B_n e^{-(n-1)\xi}\cos(n+1)\eta] \quad +$$

$$e_n[-A_n e^{-(n+1)\xi} \sin(n-1)\eta - B_n e^{(n-1)\xi}\sin(n+1)\eta] \quad +$$

$$f_n[A_n e^{-(n+1)\xi}\sin(n-1)\eta + B_n e^{-(n-1)\xi}\sin(n+1)\eta] \quad +$$

$$g_n[-\frac{1}{2\mu}\, ne^{n\xi}\cos n\eta] \quad +$$

$$h_n[\frac{1}{2\mu}\, ne^{n\xi}\cos n\eta] \quad +$$

$$j_n[-\frac{1}{2\mu}\, ne^{-n\xi} \sin n\eta] \quad +$$

$$k_n[\frac{1}{2\mu} ne^{-n\xi}\sin n\eta] \quad +$$

$$a_o[-\frac{1}{2\mu}]$$

Similarly

$$\frac{u_\eta}{h} = \sum_{n=0}^{\infty} \quad c_n[B_n e^{(n+1)\xi}\sin(n-1)\eta + A_n e^{(n-1)\xi}\sin(n+1)\eta] \quad +$$

$$d_n[B_n e^{-(n+1)\xi}\sin(n-1)\eta + A_n e^{-(n-1)\xi}\sin(n+1)\eta \;] \quad +$$

$$e_n[-B_n e^{(n+1)\xi}\cos(n-1)\eta - A_n e^{(n-1)\xi}\cos(n+1)\eta] \quad +$$

$$f_n[-B_n e^{-(n+1)\xi}\cos(n-1)\eta - A_n e^{-(n-1)\xi}\cos(n+1)\eta] +$$

$$g_n[\frac{1}{2\mu}\, ne^{n\xi}\sin n\eta] \quad +$$

$$h_n[\frac{1}{2\mu}\, ne^{-n\xi}\sin n\eta] \quad +$$

$$j_n[-\frac{1}{2\mu}\, ne^{n\xi}\cos n\eta] \quad +$$

$$k_n[-\frac{1}{2\mu} ne^{-n\xi}\cos n\eta] \ +$$

$$b_o[-\frac{1}{2\mu}] \tag{41}$$

where

$$A_n = [(n-1)\lambda' + (n-3)\mu]\frac{1}{2\mu(\lambda'+\mu)} \tag{42}$$

$$B_n = [(n+1)\lambda' + (n+3)\mu]\frac{1}{2\mu(\lambda'+\mu)} \tag{42}$$

and

$$\lambda' = \lambda(1-\nu) \tag{43}$$

Now, considering Fig. 4a and 4b the following relationships can be established between cartesian and elliptical displacement functions

$$U_x = u_\xi \sin\alpha - u_\eta \cos\alpha \tag{44}$$

$$U_n = u_\xi \cos\alpha + u_\eta \sin\alpha \tag{45}$$

where u_ξ, u_η are obtained from (40), (41) and $\sin\alpha$, $\cos\alpha$ from (15).

II.4. THE OVERDETERMINED COLLOCATION METHOD

The numerical method which will be employed for the determination of the unknown coefficients in the stress and displacement equations previously obtained is called the 'overdetermined collocation procedure'. This method is briefly described and used in [4].

Assume that (m+1) points are available on a cartesian plane, i.e.

$$(x_j, y_j) \; ; \; j = 0, 1, 2, \ldots, m$$

A 'mean curve' g(x) can be fitted through these points which will be the general form

$$g(x) \sim \sum_{j=0}^{n} a_i x^i \qquad (46)$$

where $n < m$.

So, the problem is now to determine the n+1 unknowns σ_i. Define an error quantity E as follows

$$E = \text{error square} = \sum_{j=0}^{m} [y_j - g(x_j)]^2 \qquad (47)$$

The objective will be the minimization of this error (otherwise known as the least square criterion).

Therefore,

$$\frac{\partial E}{\partial a_k} = 0; \; k = 0, 1, 2, \ldots, n \qquad (48)$$

From (48) due to (47)

$$2 \sum_{j=0}^{m} [y_i - g(x_j)] \frac{\partial g(x_j)}{\partial a_k} = 0$$

$$\sum_{j=0}^{m} [y_j - \sum_{i=0}^{n} a_i x_j^i] x_j^k = 0 \text{ for } k = 0, 1, \ldots, n$$

So,

$$\sum_{j=0}^{m} \sum_{i=0}^{n} a_i x_j^i x_j^k = \sum_{j=0}^{m} y_j x_j^k \quad \text{or}$$

$$\sum_{i=0}^{n} [\sum_{j=0}^{m} x_j^{i+k}] a_i = b_k; \; k = 0, 1, 2, \ldots, n \tag{49}$$

Now call

$$\sum_{j=0}^{m} x_j^{i+k} = c_{ki} \tag{50}$$

Therefore (49) is transformed into

$$\sum_{i=0}^{n} c_{ki} a_i = b_k \tag{51}$$

This however is a system of n+1 simultaneous equations in n+1 unknowns a_i.

Now, define a 'Vandermonde' matrix in the following way

$$A = \begin{matrix} x_0^0 & x_0^1 & \ldots\ldots & x_0^n \\ x_1^0 & x_1^1 & & x_1^n \\ x_2^0 & x_2^1 & & x_2^n \\ & & & \\ x_m^0 & x_m^1 & & x_m^n \end{matrix} \tag{52}$$

This is an (m+1) x (n+1) matrix. Therefore, it is clear that the coefficient c_{ki} defined in (50) is simply the product of the k^{th} column of A with the i^{th} column of A, or

$$c_{ki} = [A^T A]_{ki} \tag{53}$$

Therefore, multiplying (51) by A^T will yield a system of (n+1) linear simultaneous equations in (n+1) unknowns a_i.

Thus, summarizing, if the determination of N unknowns is required, M boundary points (M>N) are chosen. Then, by following the above procedure, the N unknowns are determined in such a way that the error involved in each of the N equations is a minimum.

The only remaining problem is the determination of the number of boundary points to be chosen, or, in other words, the amount by which the number of equations should exceed the number of unknowns. A useful guideline on this matter is provided by [7] where it is suggested that four or five points per half wavelength of the highest harmonic present in the series are to be used.

II.5. ANALYSIS FOR THE CASE OF TWO SYMMETRICAL HOLES

A. The stress equations

The general problem is represented in Fig. 1. In the present analysis, loading conditions that maintain symmetry about the x axis are considered while (in contrast with [21], no symmetry about the y axis is required.

So, considering Fig. 5 it is required that

$$f(X_{01}) = f(X_{02}) \text{ where } \begin{array}{l} X_{01}\ (0,\pi) \\ X_{02}\ (\pi,2\pi) \end{array} \tag{54}$$

Clearly, all cosine functions process this property (even functions) while all sine functions must be rejected as being odd. More analytically, the following table can be constructed by using odd and even multiples of cos $n\eta$ and sin $n\eta$ $(n = 1, 2, \ldots)$

Table 1

	Symmetry about x	Symmetry about y
$\cos 2n\eta$	Yes	Yes
$\cos(2n+1)\eta$	Yes	No
$\sin 2n\eta$	No	Yes
$\sin(2n+1)\eta$	No	Yes

Therefore, considering (28) and (29), the coefficients of all sine terms are set equal to 0 by following a similar reasoning with [2].

Also, from [2] the expression $c^2(\cosh 2\xi - \cos 2\eta)^2$ can be seen to have the required property. So, (28) reduces to

$$c^2(\cosh 2\xi - \cos 2\eta)^2 \sigma\xi =$$

$$\sum_{n=1}^{\infty} n \quad \cos(n+3)\eta[c_n(n+1)^{(n-1)\xi} + d_n(n+1)e^{-(n-1)\xi}] +$$

$$\cos(n+1)\eta[-4c_n e^{(n+1)\xi} - c_n(n+3)e^{(n-3)\xi} - 4d_n e^{-(n+1)\xi}$$

$$-d_n(n+3)e^{-(n-3)\xi}] +$$

$$\cos(n-1)\eta[4c_n e^{(n-1)\xi} - c_n(n-3)e^{(n+3)\xi} + 4d_n e^{-(n-1)\xi}$$

$$-d_n(n-3)e^{-(n+3)\xi}] +$$

$$\cos(n-3)\eta[c_n(n-1)e^{(n+1)\xi} + d_n(n-1)e^{-(n+1)\xi}] +$$

$$\cos(n-2)\eta[g_n(n-1)e^{n\xi} + h_n(n-1)e^{-n\xi}] +$$

$$\cos n\eta[-g_n(n-1)e^{(n+2)\xi} - g_n(n+1)e^{(n-2)\xi} - h_n(n-1)e^{-(n+2)\xi}$$

$$-h_n(n+1)e^{-(n-2)\xi}] +$$

$$\cos(n-2)\eta[g_n(n+1)e^{n\xi} + h_n(n+1)e^{-n\xi}] +$$

$$2a_o \sinh 2\xi \tag{55}$$

(29) reduces to

$$c^2(\cosh 2\xi-\cos 2\eta)^2\sigma_\eta =$$

$$\sum_{n=1}^{\infty} n \quad \cos(n+3)\eta[-c_n(n-3)e^{(n-1)\xi}-d_n(n-3)e^{-(n-1)\xi}] \; +$$

$$\cos(n+1)\eta[c_n 4e^{(n-1)\xi}+c_n(n+1)e^{(n+3)\xi}+d_n 4e^{-(n-1)\xi} \; +$$

$$d_n(n+1)e^{-(n+3)\xi}] \; +$$

$$\cos(n-1)\eta[c_n 4e^{(n-1)\xi}+c_n(n+1)e^{(n+3)\xi}+d_n 4e^{-(n-1)\xi} \; +$$

$$d_n(n+1)e^{-(n+3)\xi}] \; +$$

$$\cos(n-3)\eta[-c_n(n+3)e^{(n+1)\xi}-d_n(n+3)e^{-(n+1)\xi}] \; +$$

$$\cos(n+2)\eta[-g_n(n-1)e^{n\xi}-h_n(n-1)e^{-n\xi}] \; +$$

$$\cos n\eta[g_n(n-1)e^{(n+2)\xi}+g_n(n+1)e^{(n-2)\xi}+h_n(n-1)e^{-(n+2)\xi} +$$

$$h_n(n+1)e^{-(n-2)\xi}] \; +$$

$$\cos(n-2)\eta[-g_n(n+1)e^{n\xi}-h_n(n+1)e^{-n\xi}] \; -$$

$$2a_o \sinh 2\xi \qquad (56)$$

Finally, (30) reduces to

$$c^2(\cosh 2\xi-\cos 2\eta)^2\tau_{\xi\eta} =$$

$$\sum_{n=1}^{\infty} n \quad \sin(n+3)\eta[-c_n(n-1)e^{(n-1)\xi}+d_n(n-1)e^{-(n-1)\xi}] \; +$$

$$\sin(n+1)\eta[c_n(n+1)e^{(n-3)\xi}-d_n(n+1)e^{-(n-3)\xi}] \; +$$

$$\sin(n-1)\eta[c_n(n-1)e^{(n+3)\xi}-d_n(n-1)e^{-(n+3)\xi}] \; +$$

$$\sin(n-3)\eta[-c_n(n+1)e^{(n+1)\xi}+d_n(n+1)e^{-(n+1)\xi}] \quad +$$

$$\sin n\eta[g_n(n-1)e^{(n+2)\xi}+g_n(n+1)e^{(n-2)\xi}-h_n(n-1)e^{-(n+2)\xi} \quad +$$

$$h_n(n+1)e^{-(n-2)\xi}] \quad +$$

$$\sin(n-2)\eta[g_n(n+1)e^{n\xi}+h_n(n+1)e^{-n\xi}] \quad +$$

$$2a_o\sin 2\eta \tag{57}$$

B. <u>The displacement equations</u>

Due to the assumptions made in the previous part, the general displacement equations (40) and (41) reduce to the following forms

$$\frac{U_\xi}{h} = \sum_{n=1}^{\infty} \quad c_n[-A_n e^{(n+1)\xi}\cos(n-1)\eta-B_n e^{-(n-1)\xi}\cos(n+1)\eta] \quad +$$

$$d_n[A_n e^{-(n+1)\xi}\cos(n-1)\eta+B_n e^{-(n-1)\xi}\cos(n+1)\eta] \quad +$$

$$g_n[-\frac{1}{2\mu}\, ne^{n\xi}\cos n\eta] \quad +$$

$$h_n[\frac{1}{2\mu}\, ne^{-n\xi}\cos n\eta] \quad +$$

$$a_o[-\frac{1}{2\mu}] \tag{58}$$

and also,

$$\frac{U_\eta}{h} = \sum_{n=1}^{\infty} \quad c_n[B_n e^{(n+1)\xi}\sin(n-1)\eta+A_n e^{(n-1)\xi}\sin(n+1)\eta] \; +$$

$$d_n[B_n e^{-(n+1)\xi}\sin(n-1)\eta+A_n e^{-(n-1)\xi}\sin(n+1) \quad] \; +$$

$$g_n[\frac{1}{2\mu}\, ne^{n\xi}\sin n\eta]$$

$$h_n[\frac{1}{2\mu}\, ne^{-n\xi}\sin n\eta] \tag{59}$$

C. <u>The boundary conditions</u>

Considering one quarter of the plate only (due to symmetry reasons) and after having chosen the center of the hole as origin (for the reason of easier calculations) as shown in Fig. 6, the boundary conditions applying to the particular case are the following:

1. At $\xi = \xi_0$

$$\sigma_\xi = 0$$

$$\tau_{\xi\eta} = 0 \tag{60}$$

2. At $x = \frac{Wx}{2} - a - \frac{\ell}{2}$, $0 \leq y \leq \frac{Wy}{2}$

$$\tau_{xy} = 0$$

$$\sigma_x = \sigma_1 \tag{61}$$

3. At $y = \frac{Wy}{2}$, $-(\frac{\ell}{2} + a) \leq x \leq \frac{Wx}{2} - a - \frac{\ell}{2}$

$$\tau_{xy} = 0$$

$$\sigma_y = \sigma_2 \tag{62}$$

4. At $x = -(\frac{\ell}{2} + a)$, $0 \leq y \leq \frac{Wx}{2}$

$$U_x = 0$$

$$\tau_{xy} = 0 \tag{63}$$

Furthermore, it will be next shown that U_y and τ_{xy} vanish identically at

$$y = 0, \; -\left(\frac{\ell}{2} + a\right) \leq x \leq \frac{Wx}{2} - a - \frac{\ell}{2}$$

From the definition of the coordinate system, at

$$0 \leq x \leq \frac{Wx}{2} a - \frac{\ell}{2}, \; y = 0 \; \eta = 0 \qquad (64a)$$

and at

$$-\left(\frac{\ell}{2} + a\right) \leq x \leq 0, \quad y = 0 \qquad \eta = \pi \qquad (64b)$$

Now, from (64a), using (15), (18) and (57) it is clear that

$$\tau_{xy} = 0 \text{ identically} \qquad (65a)$$

Also, using (15), (45) and (58), (59) it is again clear that

$$U_y = 0 \text{ identically} \qquad (65b)$$

Finally, use of (64b) and a similar reasoning as above, leads to the conclusion that (65a) and (65b) are also true for $\eta=\pi$.

It should be emphasized that in this case the conditions

$$U_y = 0; \quad \tau_{xy} = 0$$

are identically satisfied along the x axis since symmetry about this axis only was assumed. On the other hand, in [2]

$$\tau_{xy} = 0$$

$$U_y = 0 \text{ along the x axis}$$

$$U_x = 0 \text{ along the y axis}$$

were identically satisfied along both the x and y axes due to symmetry assumed about both those axes. However, displacement considerations are not explicitly stated in [2].

II.6. SELECTION OF BOUNDARY POINTS FOR THE TWO HOLE CASE

Due to [2], it was decided to truncate the series at n = 10. Therefore the problem was to determine the resulting 41 unknown (c_1 through c_{10}, d_1, through d_{10}, g_1 through g_{10}, h_1 through h_{10} and a_o) by using the overdetermined collocation method.

It was noted that the highest harmonics in the equations were cos 13η and sin 13η so that one-half wavelength was approximately 6. Thus, four times six points, as recommended in [7] would yield enough equations and consequently the number of points to be chosen was 24. This resulted in a system of 48 equations in 41 unknowns for each value of the separation of the two elliptical holes.

As shown in Fig. 7, the distribution of the points chosen was as follows:

8 points on the ellipse boundary

7 points on the outer edge x = constant

2 points on the inner edge x = constant

7 points on the outer edge y = constant

Then, the boundary conditions described in the previous chapter were satisfied at those points so that the 48 equations were formed. The method used for the determination of the elliptical coordinates of selected points on the rectangular boundaries will be next described.

Consider the boundary

$$X = \frac{Wx}{2} - a - \frac{\ell}{2}; \quad 0 < y < \frac{Wy}{2}$$

Divide the distance along the y axis into 8 equal spaces and so, the y coordinate of the k^{th} point on this edge at which the boundary conditions will be satisfied

$$Y_k = [(\frac{Wy}{2})/8]k \tag{66}$$

Now an angle is defined as follows

$$\theta = \tan^{-1}[Y_k/(x-c)] \tag{67}$$

where x is given by

$$x = \frac{Wx}{2} - a - \frac{\ell}{2}$$

and, of course,

$$c = \sqrt{a^2-b^2} \tag{68}$$

Then,

$$PB = \left| (x-c)/\cos\theta \right| \tag{69}$$

and

$$OA = \frac{1}{2}[PB + \sqrt{PB^2 + 4cx}]$$

So, if Q is defined to be

$$Q = \sqrt{1 - c^2/OA^2} \tag{71}$$

The elliptical coordinates ξ and η at that point are defined as follows

$$\xi = \frac{1}{2} \log \frac{1+Q}{1-Q} \tag{72}$$

and

$$\eta = \frac{\pi}{2} - \tan^{-1} \left[\frac{x}{OA\sqrt{1-x^2/OA}}\right] \tag{73}$$

The above method results from the definition of ξ and η in (1) and (2) and also from the geometry of the problem. A similar procedure was in [2]. Now,the values of ξ and η in the other rectangular boundaries are also defined by the above method.

Note that care has been taken not to consider any points on the edge of the boundaries because, at such corner points, the stress concentrations arising from the discontinuity present, cannot be taken into account by the theory used.

Finally, the numerical values of the plate and hole dimensions, the separation of the elliptical holes, and the loading conditions used are given below

1. <u>Plate</u>

   $W_x = 20''$ $W_y = 20''$

2. <u>Holes</u>

   $2a = 1.5''$ $2b = 0.75''$

3. <u>Separation of holes</u>

   $\ell = 0.128''; 0.192''; 0.357''; 0.748''; 1.494''; 2.938''$

4. <u>Loading</u>

   $k = 0.50; 4.00$

II.7. A BRIEF APPROACH TO THE OBLIQUE HOLE CASE

This case is the most general of the problem and can be used to analyze any type of flat plate perforated with any type and number of elliptical discontinuities and subjected to any combination of in plane loading.

Since, in such a case, there is no symmetry about any axis, it is necessary to use the equations developed in Chapters 2 and 3 since all the terms have to be included in the analysis. Therefore, the unknowns to be dealt with will now be the following

$$c, d, j, k, e, f, g, h, a_o, b_o$$

Therefore, truncation of the series at any point $n = N$ will yield

$$8N + 2$$

unknowns.

So, the next problem arising is the determination of the points where the boundary conditions will be satisfied. It is advised to partition the plate in a number of rectangular pieces equal to the number of holes present. An example of this method is demonstrated in Fig. 8. Then, the following boundary conditions are to be satisfied.

1. At all outer edges of the plate, the shear stress τ_{xy} should be equal to 0 and the appropriate direct stress (i.e., either σ_x or σ_y) should be equal to the external loading.

2. On all ellipse boundaries, σ_ξ and $\tau_{\xi\eta}$ must be equal to zero.

3. On all inner cuts (see Fig. 8) compatibility of displacements is also required.

Consequently, imposing 1, 2, 3 and chosing an adequate number of points according to [7], enough equations can be formed so that employment of the overdetermined collocation method will yield the required unknowns. Thus, the stresses (and hence the stress concentration factors) can be obtained at points of interest.

The two important aspects to be considered however, before any calculations are carried out as follows:

A. <u>The convergence of the series</u>

The series used for the various stress components is not always well behaved. As a matter of fact, the coefficients of c, g, j, e diverge very rapidly as the terms are multiplied by exponentials (e.g., $e^{n\xi}$), while the coefficients of d, g, k, f converge practically after the third or fourth terms as they contain rapidly increasing powers of e in the denominator. So, it is necessary to truncate the series at various points and test for the convergence of the resulting numerical values. This can be done rather easily, by modifying the computer program developed as described in the next section of this thesis.

However, the analysis in [2] as well as the results obtained for the particular case under consideration, indicate that a truncation of the series at $n = 10$ will yield acceptable results.

B. The location and number of boundary points

Although it is good practice to chose a number of boundary points greater than that of unknowns, it is equally important not to produce too many equations, because the subsequent increase in the least square error associated with the collocation method will reduce the credibility of the results obtained.

Again, as a result of the observations carried out in [7], [2], as well as the present analysis, the abovementioned recommended number of (4 x half wavelength of highest unknown present in series) should be used when decided on the boundary points.

Finally, care should be taken not to consider any points at odd locations such as plate edges etc., because various stress concentrations and other external factors arise that will have a marked influence which is difficult to quantify.

Now, the theory is general enough to include any type of elliptical discontinuities on the plates. However, due to the derivation of the value of

$$\xi = \tanh^{-1} \frac{b}{a} \qquad (74)$$

the limiting case when the ellipses become circles cannot be considered as $\xi \to \infty$. Of course, it is wise not to try to use this method if the ratio

$$\frac{b}{a} \to 1$$

On the other hand, it is possible to consider the other limiting case when the ellipses become cracks (i.e., $b = 0$). Then $\xi = 0$ and $c = a$. Therefore, it is easy to appreciate the usefulness of this method for the calculation of stress concentrations due to cracks in plates.

SECTION III

THE COMPUTER PROGRAM

III.1. GENERAL STRUCTURE

As stated earlier, a computer program was developed using as input

(a) The dimensions of the plate

(b) The dimensions of the hole

(c) The loading conditions

(d) The separation of the elliptical holes

(e) Poisson's ratio ν

which prints out the stress component σ_η at various required points on the ellipse boundary. The calculation of the various coefficients and the solutions of the resulting systems of equations are done by the program and it is possible to consider any combination or combinations of the input parameters in one run, thus minimizing compilation costs.

Analytically, the program performs the following functions after input is read and printed out:

1. Calculates ξ_o which is the value of ξ at any point on the elliptical boundary

2. Using purely geometrical considerations, the values of the eccentric angle η is calculated at various points on the ellipse boundary

3. Using these values of ξ_o and η the values of the coefficients of the unknowns in σ_ξ and $\tau_{\xi\eta}$ are calculated at those points, using subroutines COINT 1, COINT 2 and COINT 3. (See Appendix 2). So, a matrix A is formed.

4. Next, using the technique described in the previous section, the values of ξ and η are calculated on the outer edges of the plate.

5. Using the values of the elliptical coordinates previously obtained, the coefficients of the unknown constants in σ_x, σ_y and τ_{xy} at those points are calculated using EXT 1, EXT 2 and EXT 3 (see Appendix 2). So, matrices B and BB are formed from the conditions on the outer edge x = constant and the outer edge y = constant respectively.

6. The values of ξ and η are determined at selected points on the inner edge x = constant and the coefficients of the unknown constants in τ_x and τ_{xy} are calculated using EXT 4X and EXT 1 respectively (see Appendix 2). Consequently the matrix DX is formed.

7. The matrix AA is formed from A, B, BB and DX - AA is the general LHS of the system to be formed.

8. The RHS matrix of the system QJ is also formed.

9. The transpose of AA is obtained by the use of subroutine GMTRA and then the products $[AA^T\ AA]$ as well as $[AA^T\ QJ]$ are formed by subroutine GMPRD.

10. After the completion of the previous step, the system of simultaneous equations formed is solved by subroutine SIMQ. It is advisable, to use, at least during the first run of the program, subroutine GMPRD as a double check of the solution obtained by SIMQ. The values of the solutions thus obtained are stored in the original RHS vector QJ.

11. Using the values of the constants obtained in the previous step, σ_η is now determined at various locations of the ellipse boundary, so that the stress concentrations at those points can be determined.

12. Steps 1 through 11 are repeated for each new value of ℓ.

Finally, there are the following points to be observed in the computer program:

(a) The values of the coefficients of the unknowns are shared in labelled COMMON BLOCKS between the main program and the appropriate subroutines. In this way easier (and hence cheaper) communication between subprograms or subprograms and main is achieved. Also, in this way it is not necessary to include those coefficients in the subroutine parameters.

(b) Subroutines SIMQ, GMPRD and GMTRA must have vectors and not two-dimensional matrices as input. This obstacle is overcome by the use of EQUIVALENCE statements which effectively transform the two-dimensional matrices obtained at the various steps to one-dimensional.

(c) Subroutine SIMQ has a built-in control against overflow, in the form of KS. So, if the matrix to be solved is singular, the value of 1 is printed out for KS and calculations automatically stop; otherwise, the value of 0 is printed for KS. Therefore, it was not considered necessary to incorporate any additional control statments for this case.

III.2. ALTERATIONS TO ADJUST FOR OTHER CASES

Although the computer program as used here is general enough, the following alterations can be easily made to adjust for other cases.

1. In order to consider any number of plates, holes, separations and loading conditions, the general input entry form can take the following format:

```
252  READ (5,500) SA, SB, AO, BO
     IF (SA.EQ.0.0) STOP
     WRITE (6,602) SA, SB, AO, BO
251  READ (5,501) SXX, SYY
     IF (SXX.EQ.0.0) GO TO 252
     AKAPA = SYY/SXX
     WRITE (6,603) SXX, SYY, AKAPA
250  READ (5,502) BLGM
     IF (BLGM.EQ.0.0) GO TO 251
     WRITE (6,604) BLGM
```

Thus, using the above control statements, it can be seen that ℓ is at the lowest control level so that if the last value is set to 0.0 the program will transfer control to a new set of loading conditions. Then, at this second control level, is σ_x is set to zero, a new plate will be examined. Finally, setting the last value of 'a' equal to 0 will simply stop execution and therefore this technique can be used as an alternative to the CALL EXIT statement.

2. To change the number of boundary points considered it is only necessary to change the limit of the DO loops calculating the values of ξ and η at various points on the plate as well as the values of the steps used at those DO loops. In such a case the number of equations will change while the number of unknowns will remain the same. So, it is necessary to change the DIMENSION statements in an appropriate way.

3. To change the number of points at which the series are truncated, the upper limit of the DO loops in the subroutines has to be changed. In such a case however, since the number of unknowns will be altered, it might be necessary to change the number of boundary points so that the procedure in 2 is also to be repeated. Of course, in both 2 and 3 the matrix formation statements in the main program must be also altered.

Finally, some form of 'book keeping' is advised during any attempt of alteration of the program so as to avoid duplicate statement labels or similar errors. It should also be noted that the complier at which this program was run permited the use of mixed type expressions (i.e., integer and real). This is not the case for all compilers however, so that the need to use FLOAT or INT statements to bring about compatibility in the various expression may arise.

SECTION IV

RESULTS AND CONCLUSIONS

IV-1. RESULTS

Using the computer program described in the previous section, a first set of results for stress concentrations at $\eta = 0$ and $\eta = \pi$ was obtained. These results are shown in the following tables and also in Graphs 1 through 4. The experimental results are also shown (as obtained in [2]) since the main object was the comparison of the two sets of results.

Table IV-1

$S = (\sigma_\eta/\sigma_2)_{\eta=0}$; $K = 0.5$; $a/b = 2$

ℓ	S (theoretical)	S (experimental
0.128	4.07	3.76
0.192	3.43	3.40
0.357	3.68	3.23
0.748	3.33	3.29
1.494	3.21	2.86
2.983	3.76	3.22

It is obvious from the above table and also from Graph 1 that the theoretical results lie on both sides of the experimental. Variation however is such, that mean curves passed through both sets of results will almost coincide. The only exception is the result obtained for $\ell = 2.983$ but this was probably due to some numerical inaccuracy resulting from the solution of the simultaneous equations.

Table IV-2

$S = (\sigma_\eta/\sigma_{2_\eta})_\pi$; K = 0.5; a/b = 2

ℓ	S (theoretical)	S (experimental)
0.128	7.38	7.10
0.192	5.75	5.77
0.357	4.96	4.65
0.748	4.21	3.47
1.494	3.68	2.81
2.983	3.61	3.22

As shown in the above table and also Graph 2, the theoretical results are, except in the case of ℓ = 0.192" higher than the experimental but the slopes of the curves passing through these two sets are almost identical.

From the two above cases, it was observed that there existed an acceptable agreement of theoretical and experimental results, and this verified the theory developed in Section II and the computer program developed in Section III of this thesis.

However, to gain further confidence to the numerical method, a second set of results was obtained for K = 4.0. These are shown in Tables IV-3 and IV-4 and also in Graphs 3 and 4.

Table IV-3

$S = (\sigma_\eta/\sigma_2)_{\eta=0}$; K = 4.0; a/b = 2

ℓ	S (theoretical)	S (experimental)
0.128	5.25	4.94
0.192	4.95	5.02
0.357	4.52	4.68
0.748	4.36	4.03
1.494	4.4]	4.14
2.983	4.55	4.41

Table IV-4

$S = (\sigma_\eta/\sigma_2)_{\eta=\pi}$; K = 4.0; a/b = 2

ℓ	S (theoretical)	S (experimental)
0.128	8.03	7.77
0.o92	7.51	7.44
0.357	4.78	5.33
0.748	4.46	4.20
1.494	4.44	4.23
2.983	4.48	4.26

So, it is clear that this second sec of theoretical results is in even closer agreement with the experiments and this gives further confidence to the numerical method, at least if absolute accuracy is not required but only an indication of the region of a particular value.

The next item to be tested was the sensitivity of the overdetermined collocation method to the number of boundary positions chosen. So, by fixing the value of ℓ to 1.494" the aspect ratio a/b to 2, the value of K to 0.5 and finally truncating the series at n = 10, the value of S and $\eta=0$ and $\eta=\pi$ was calculated for 22, 24, 26, 28, 30 and 34 points. The results were plotted in Graphs 5 and 6 respectively.

The first observation to be made in both graphs is that the results are rather significantly sensitive to the amount of overdetermination of the method but there is a marked flat region from 24 to 28 points, in both cases, in which the results are almost identical. Since the highest harmonic wavelength in the series was 13, this region corresponds to about 4 points per half wavelength, a conclusion which exactly checks with that in [7]. It should be emphasized however, that if the results are not obtained within this acceptable region, then there is very little confidence in their validity. This happens because, beyond a certain degree of overdetermination, the square error involved increases significantly to reduce the accuracy of the results.

The next test to be carried out was the sensitivity of the series to truncation. The parameters kept constant during this test were the following:

(a) ℓ = 1.494"

(b) a/b = 2

(c) k = 0.5

(d) 4 points per half wavelength of the highest hamonic in the series were used.

Again, two sets of results were obtained for η=0 and η=π which are plotted in Graphs 7 and 8 respectively. The results here are similar to those obtained in the previous case since there is again a flat region from n=6 to n-10 in which the results are almost unaffected by the point at which the series is truncated. This is quite important because truncation of the series at the lowest possible point will result in fewer unknowns and will thus save on computer time. Beyond n=10 however, the rapidly diverging coefficients of c_n and g_n cause a divergence of the series and this is the reason why the accuracy of the results deteriorates rapidly beyond that point.

The final set of results to be obtained consisted of a check of the effect of a and b on S. The parameters kept fixed during this test were the following:

(a) $\eta = \pi$ since greater stress concentrations were observed here than in the case of $\eta = 0$.

(b) K = 0.5

Three new sets of a and b were considered, namely

$$a/b = 8$$

$$a/b = 4$$

$$a/b = 1.5$$

and the results are shown in Graph 9. It is clear that in all cases there is a value of ℓ, beyond which the interaction becomes unimportant. As a rough indication of this value, one can assume ℓ = 0.75 to 1.10 times the semimajor diameter.

It can be seen that the value of S after the interaction between the two ellipses has ceased is in a rather distinct relationship with the theoretical prediction for an elliptical hole in an infinite plate.

Since this value is

$$S = 1 + 2\frac{a}{b}$$

when loading is uniaxial and parallel to b, for K = 0.5, by regarding biaxial loading as the superposition of two uniaxial loading conditions we get the following results

a/b	Theoretical	Experimental
1.5	3.44	3.00
2.0	4.00	5.00
4.0	7.00	8.80
8.0	11.75	11.00

So, a rough indication of the value of S can be obtained, without using the program, provided that ℓ is greater than 1.1a

IV-2. CONCLUSIONS

1. The numerical method gives acceptable accuracy as compared to the experimental results.

2. The optimum number of boundary points for the overdetermined collocation method is four points per half wavelength of the greatest harmonic present in the series.

3. The optimum point for the truncation of the particular series used is between n=6 and n=10.

4. The distance at which interaction between elliptical discontinuities becomes unimportant is approximately 0.75 to 1.10 times the semimajor diameter. Beyond that point, a rough indication for the value of S is obtained by the theoretical method described in the previous chapter.

IV-3. RECOMMENDATIONS

1. It would be interesting to compare the method used with the finite element method from the points of view of accuracy and expense.

2. The application of the method to a 3-D problem similar to the one considered here would be rather easy to handle.

3. A more detailed examination of the oblique hole case could provide the most general results.

APPENDIX 1

MODIFICATION OF EQUATIONS FOR COMPUTER USE

The equations for the various stress components, both elliptical and rectangular as developed in the theoretical part of this thesis are not suitable for use by the computer. Therefore, they are modified in the following way, by rearranging terms as coefficients of the unknown constants.

$$c^2(\cosh 2\xi - \cos 2\eta)^2 \sigma\xi =$$

$$\sum_{n=1}^{\infty} \quad c_n n[(n+1)e^{(n-1)\xi}\cos(n+3)\eta - 4e^{(n+1)\xi}\cos(n+1)\eta -$$

$$(n+3)e^{(n-3)\xi}\cos(n+1)\eta - (n-3)e^{(n+3)\xi}\cos(n-1)\eta +$$

$$4e^{(n-1)\xi}\cos(n-1)\eta + (n-1)e^{(n+1)\xi}\cos(n-3)\eta] +$$

$$d_n n[(n+1)e^{-(n-1)\xi}\cos(n+3)\eta - 4e^{-(n+1)\xi}\cos(n+1)\eta -$$

$$(n+3)e^{-(n-3)\xi}\cos(n+1)\eta + 4e^{-(n-1)\xi}\cos(n-1)\eta -$$

$$(n-3)e^{-(n+3)\xi}\cos(n-1)\eta + (n-1)e^{-(n+1)\xi}\cos(n-3)\eta] +$$

$$g_b n[(n+1)e^{n\xi}\cos(n+2)\eta - (n-1)e^{(n+2)\xi}\cos n\eta -$$

$$(n+1)e^{(n-2)\xi}\cos n\eta + (n+1)e^{n\xi}\cos(n-2)\eta] +$$

$$h_n n[(n-1)e^{-n\xi}\cos(n\pm 2)\eta - (n-1)e^{-(n+2)\xi}\cos n\eta -$$

$$(n+1)e^{-(n-2)\xi}\cos n\eta + (n+1)e^{-n\xi}\cos(n-2)\eta]$$

$$+ 2a_o \sinh 2\xi$$

Similarly,

$$c^2(\cosh 2\xi-\cos 2\eta)^2\sigma_\eta =$$

$$\sum_{n=1}^{\infty} \quad c_n n[-(n-3)e^{(n-1)\xi}\cos(n+3)\eta-4e^{(n+1)\xi}\cos(n+1)\eta +$$
$$(n-1)e^{(n-3)\xi}\cos(n+1)\eta+4e^{(n-1)\xi}\cos(n-1)\eta +$$
$$(n+1)e^{(n+3)\xi}\cos(n-1)\eta-(n+3)e^{(n+1)\xi}\cos(n-3)\eta] \quad +$$

$$d_n n[-(n-3)e^{-(n-1)\xi}\cos(n+3)\eta-4e^{-(n+1)\xi}\cos(n+1)\eta +$$
$$(n-1)e^{-(n-3)\xi}\cos(n+1)\eta+4e^{-(n-1)\xi}\cos(n-1)\eta +$$
$$(n-1)e^{-(n+3)\xi}\cos(n-1)\eta-(n+3)e^{-(n+1)\xi}\cos(n-3)\eta] +$$

$$g_n n[-(n-1)e^{n\xi}\cos(n+2)\eta+(n-1)e^{(n+2)\xi}\cos n\eta +$$
$$(n+1)e^{(n-2)\xi}\cos n\eta-(n+1)e^{n\xi}\cos(n-2)\eta] +$$

$$h_n n[-(n-1)e^{-n\xi}\cos(n+2)\eta+(n-1)e^{-(n+2)\xi}\cos n\eta +$$
$$(n+1)e^{-(n-2)\xi}\cos n\eta-(n+1)e^{-n\xi}\cos(n-2)\eta] \quad +$$

$$2a_o \sinh 2\xi$$

Finally,

$$c^2(\cosh 2\xi-\cos 2\eta)^2\tau_{\xi\eta} =$$

$$\sum_{n=1}^{\infty} \quad c_n n[-(n-1)e^{(n-1)\xi}\sin(n+3)\eta+(n+1)e^{(n-3)\xi}\sin(n+1)\eta +$$
$$(n-1)e^{(n+3)\xi}\sin(n-1)\eta-(n+1)e^{(n+1)\xi}\sin(n-3)\eta] +$$

$$d_n n[(n-1)e^{-(n-1)\xi}\sin(n+3)\eta-(n+1)e^{-(n-3)\xi}\sin(n+1)\eta -$$
$$(n-1)e^{-(n+3)\xi}\sin(n-1)\eta+(n+1)e^{-(n+1)\xi}\sin(n-3)\eta] +$$

$$g_n n[-(n-1)e^{n\xi}\sin(n+2)\eta + (n-1)e^{(n+2)\xi}\sin n\eta +$$
$$(n+1)e^{n\xi}\sin(n-2)\eta + (n+1)e^{(n-2)\xi}\sin n\eta] +$$
$$h_n n[(n-1)e^{-n\xi}\sin(n+2)\eta - (n-1)e^{-(n+2)\xi}\sin n\eta -$$
$$(n+1)e^{-(n-2)\xi}\sin n\eta + (n+1)e^{-n\xi}\sin(n-2)\eta\ ] +$$
$$2a_o\sin 2\eta$$

It was also found necessary to rearrange in a similar way the equations for σ_x, σ_y and τ_{xy}.

In the subsequent equations,the notation used is the following:

CC1, DD1, GG1, HH1 and A01 are the coefficients of c_n, d_n, g_n, h_n and a_o respectively in σ_ξ CC3, DD3, GG3, HH3 and A03 are the coefficients of c_n, d_n, g_n, h_n and a_o respectively in σ_η, while subscrip 2 refers to $\tau_{\xi\eta}$

Thus,

$$c^2(\cosh 2\xi - \cos 2\eta)^2\sigma_x =$$

$$\sum_{n=1}^{\infty} c_n[\text{CC1}\sin^2\alpha + \text{CC3}\cos^2\alpha - \text{CC2}\sin 2\alpha] +$$
$$d_n[\text{DD1}\sin^2\alpha + \text{DD3}\cos^2\alpha - \text{DD2}\sin 2\alpha] +$$
$$g_n[\text{GG1}\sin^2\alpha + \text{GG3}\cos^2\alpha - \text{GG2}\sin 2\alpha] +$$
$$h_n[\text{HH1}\sin^2\alpha + \text{HH3}\cos^2\alpha - \text{HH2}\sin 2\alpha] +$$
$$a_o[\text{A01}\sin^2\alpha + \text{A03}\cos^2\alpha - \text{A02}\sin 2\alpha]$$

Similarly,

$$c^2(\cosh 2\xi-\cos^2\eta)^2\ \sigma_y =$$

$$\sum_{n=1}^{\infty}\ c_n[CC1\cos^2\alpha + CC3\sin^2\alpha + CC2\sin 2\alpha] +$$

$$d_n[DD1\cos^2\alpha + DD3\sin^2\alpha + DD2\sin^2\alpha] +$$

$$g_n[GG1\cos^2\alpha + GG3\sin^2\alpha + GG2\sin^2\alpha] +$$

$$h_n[HH1\cos^2\alpha + HH3\sin^2\alpha + HH2\sin 2\alpha] +$$

$$a_o[AO1\cos^2\alpha + AO3\sin^2\alpha + AO2\sin 2\alpha]$$

and finally

$$c^2(\cosh 2\xi-\cos 2\eta)^2\ \tau_{xy} =$$

$$\sum_{n=1}^{\infty}\ c_n[0.5(CC1-CC3)\sin 2\alpha - CC2\cos 2\alpha] +$$

$$d_n[0.5(DD1-DD3)\sin 2\alpha - DD2\cos 2\alpha] +$$

$$g_n[0.5(GG1-GG3)\sin 2\alpha - GG2\cos 2\alpha] +$$

$$h_n[0.5(HH1-HH3)\sin 2\alpha - HH2\cos 2\alpha] +$$

$$a_o[0.5(AO1-AO3)\sin 2\alpha - AO2\cos 2\alpha]$$

Now, using the formulae linking rectangular and elliptical displacements an expression for U_x similar to the above was obtained. So,

$$\frac{U_x}{h} = \sum_{n=1}^{\infty}\ c_n[CC7\sin\alpha - CC8\cos\alpha] +$$

$d_n[DD7\sin\alpha - DD8\cos\alpha]$ +

$g_n[GG7\sin\alpha - GG8\cos\alpha]$ +

$h_n[HH7\sin\alpha - HH8\cos\alpha]$ +

$a_o[AO7\sin\alpha - AO8\cos\alpha]$

Note that

CC7, DD7, GG7, HH7, AO7 are the coefficients of c_n, d_n, g_n, h_n and a_o respectively in U_ξ CC8, DD8, GG8, HH8, AO8 are the coefficients of c_n, d_n, g_n, h_n and a_o respective in U_η.

Now, the values of E and ν used in [2] were not available. Therefore a typical value of 0.36 for ν was assumed while E was simplified out of the displacement equations since, at the boundary points considered, the RHS of those equations was equal to zero.

In this way the error from assuming an arbitrary numerical value for E was minimized while, on the other hand, the coefficients of the displacement equations were decreased by several orders of magnitude, thus reducing the computer time required for the calculations. Of course, if it were necessary to determine the displacements at any arbitrary point (and not along the boundary) the value of E would be included since the RHS of the equation would be unknown.

APPENDIX 2

BRIEF DESCRIPTION OF SUBROUTINES

A brief description of the subroutines used is provided in this appendix although some discussion is also included in Section III.

Subroutines COINT 1, COINT 2 and COINT 3 are used to calculate the coefficients of the unknown constants in σ_ξ, $\tau_{\xi\eta}$ and σ_η respectively. This is done by two DO loops whose upper limit indicates the value of n at which the series is truncated. If the nature of the problem is such that requires separate calculation of odd and even terms in those coefficients, then a DO loop can be used for each of these calculations. This was actually the reason for providing two instead of one DO loops. The input parameters of these subroutines are I (the number of points on a specified boundary on which the coefficients are to be calculated), SI (the value of ξ on each of the I points of that boundary) and ETA (the value of η on each of the I points of that boundary. The values of the calculated coefficients of the unknown constants are not included as SUBROUTINE parameters but are shared in a COMMON file by the main program and subroutines EXT 1, EXT 2 and EXT 3.

Subroutine TRIG 2 calculates the angle α necessary to transform from elliptical into cartesian coordinates. The input parameters are M (the number of points on a specified boundary on which the coefficients are to be calculated, SSI (the value of ξ at each of the M points) and HTA (the value of at those specified points). The values of $\sin\alpha$, $\sin2\alpha$, $\cos\alpha$, $\cos2\alpha$ obtained are shared in a COMMON file by subroutines TRIG2, EXT1, EXT2, EXT3 and EXT4X.

Subroutines EXT1, EXT2 and EXT3 are provided for the calculation of the coefficients of the unknown constants in the cartesian stress expressions τ_{xy}, σ_x and σ_y respectively. This is done by the use of COINT1, COINT2 and COINT3, using also the results obtained in TRIG2. The values of the calculated coefficients are shared in COMMON files with the main program.

Subroutines DIS1KS and DIS2HT calculate the values of the coefficients of the unknown constants in U_ξ and U_η respectively. The input parameters are similar to those of the first three subroutines, while the results obtained are shared in COMMON files with EXT4X.

Subroutine EXT4X calculates the values of the coefficients of the unknown constants in U_x. This is done by using the two previously described subroutines as well as TRIG2. The results obtained are shared in a COMMON file with the main program.

Finally, subroutines GMPRD, GMTRA and SIMQ are described in [8].

APPENDIX 3

COMPUTER NOMENCLATURE

Compare the symbols on the right hand side with 'NOMENCLATURE', page

SA	=	a
SB	=	b
AO	=	W_x
BO	=	W_y
SXX	=	σ_x
SYY	=	σ_y
AKAPA	=	K
BLGM	=	ℓ
C	=	c
SKO	=	ξ_o
SKSI, SI, XI	=	ξ
F, HTA, ETA, TA	=	η
SIGETA	=	σ_η

APPENDIX 4

DEVELOPMENT OF DISPLACEMENT FUNCTIONS

The general displacement functions were obtained from [3] as mentioned in Section II of this thesis. An explicit example of the procedure used is described below.

Consider the following four components of the general stress function used in [3]

$$\psi_1 = \cosh n\xi \cos n\eta \tag{5-1}$$

$$\psi_2 = \sinh n\xi \sin n\eta \tag{5-2}$$

$$\psi_3 = \sinh n\xi \cos n\eta \tag{5-3}$$

$$\psi_4 = \cosh n\xi \sin n\eta \tag{5-4}$$

Also consider four of the components used in the stress function Φ as described in Section II

$$\Phi_5 = e^{n\xi} \cos n\eta \tag{5-5}$$

$$\Phi_6 = e^{-n\xi} \cos n\eta \tag{5-6}$$

$$\Phi_7 = e^{n\xi} \sin n \tag{5-7}$$

$$\Phi_8 = e^{-n\xi} \sin n\eta \tag{5-8}$$

So, from (5-1) through (5-8) the following relations can be proved to be true

$$\Phi_5 = \psi_1 + \psi_3 \tag{5-9}$$

$$\Phi_6 = \psi_1 - \psi_3 \tag{5-10}$$

$$\Phi_7 = \psi_2 + \psi_4 \tag{5-11}$$

$$\Phi_8 = \psi_4 - \psi_2 \tag{5-12}$$

Now, from p. 197 [3], by considering the displacement functions corresponding to ψ_1 and ψ_3, the displacement function corresponding to Φ_5 can be obtained, using (5-9); thus, for Φ_5

$$\frac{U_\xi}{h} = -\frac{1}{2\mu} n\ [\sinh n\xi + \cosh n\xi] \cos n\eta$$

$$= -\frac{1}{2\mu} n\ [\frac{1}{2}\ (e^{n\xi}-e^{-n\xi}+e^{n\xi}+e^{-n\xi}]\ \cos n\eta$$

$$= -\frac{1}{2\mu} ne^{n\xi}\cos n\eta \qquad (5\text{-}13)$$

Also

$$\frac{U_\eta}{h} = \frac{1}{2\mu} n[\cosh n\xi + \sinh n\xi]\ \sin n\eta$$

$$= \frac{1}{2\mu} ne^{n\xi}\sin n\eta \qquad (5\text{-}14)$$

In a similar way, the displacement functions corresponding to all other components of the stress function Φ are obtained.

Of course all these expressions were subsequently checked by integration against the already existing stress functions and were found to be in agreement. In this way the possibility of misprints in the equations of [3] was ruled out.

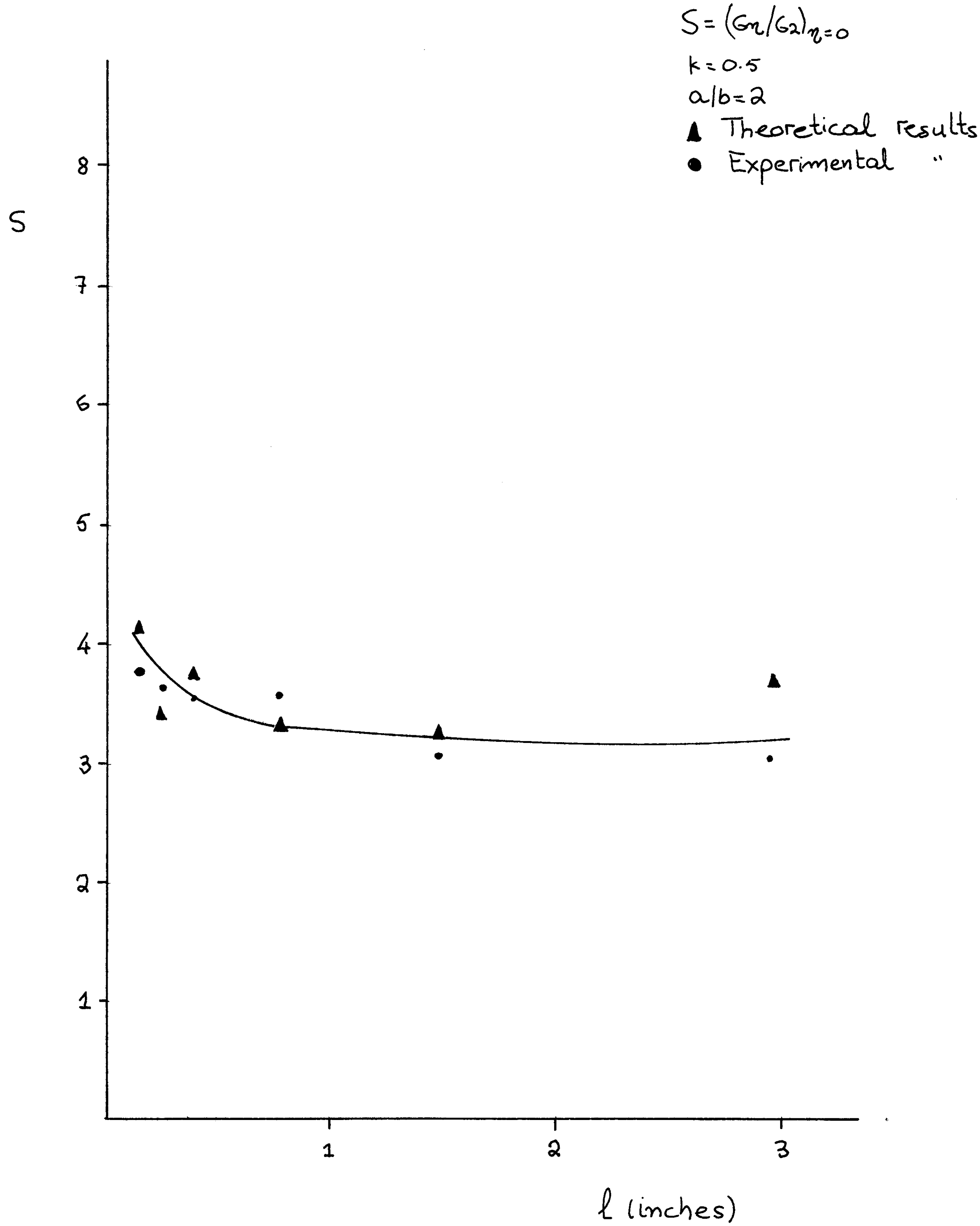
S = (σr/σ2)η=0
k = 0.5
a/b = 2
Theoretical results
Experimental "
S
8
7
6
5
4
3
2
1
1
2
3
l (inches)

GRAPH 1

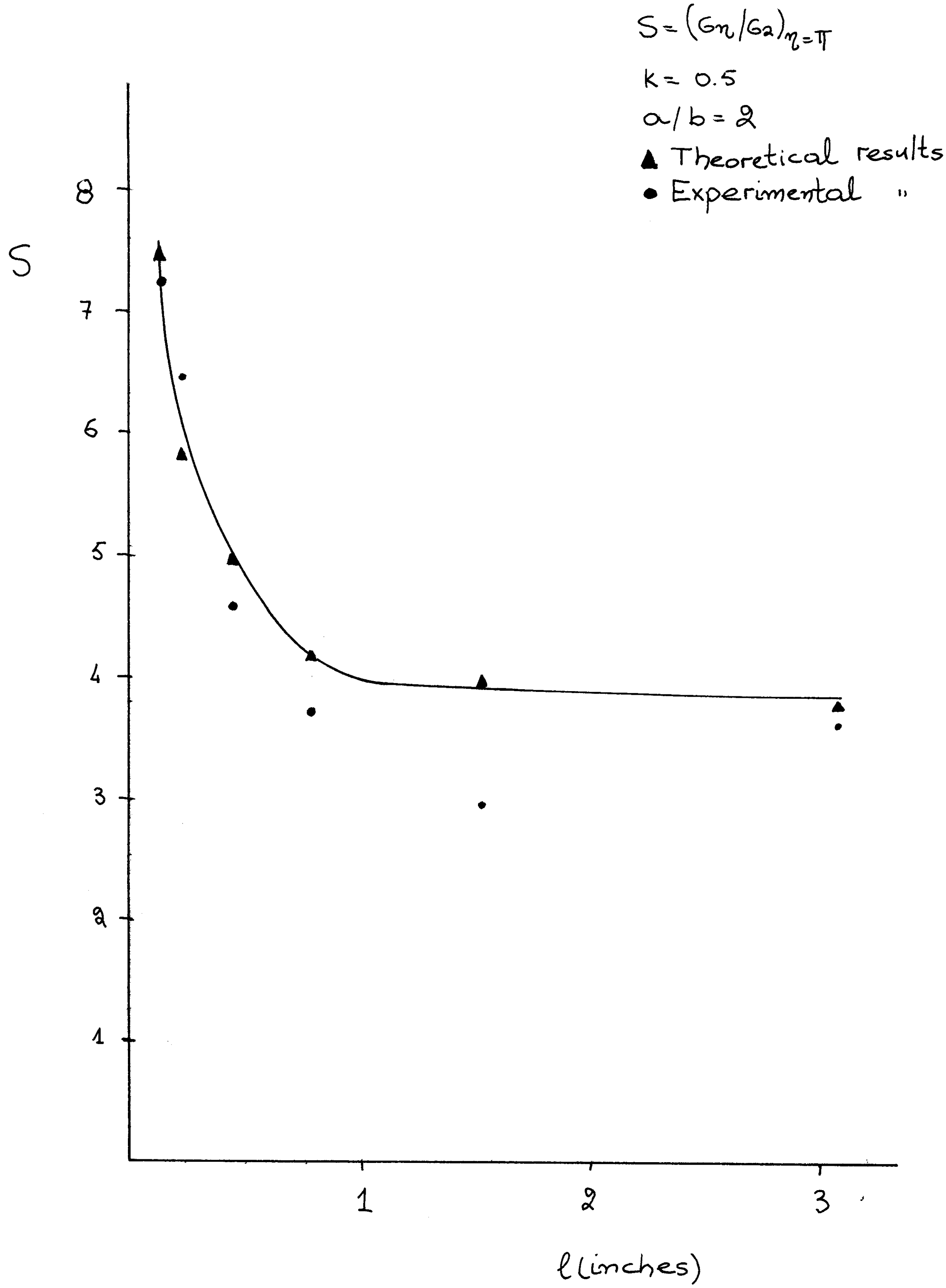

S = (Gn/Ga)η=π
k = 0.5
a/b = 2
▲ Theoretical results
● Experimental "
S
8
7
6
5
4
3
2
1
1
2
3
l (inches)

GRAPH 2

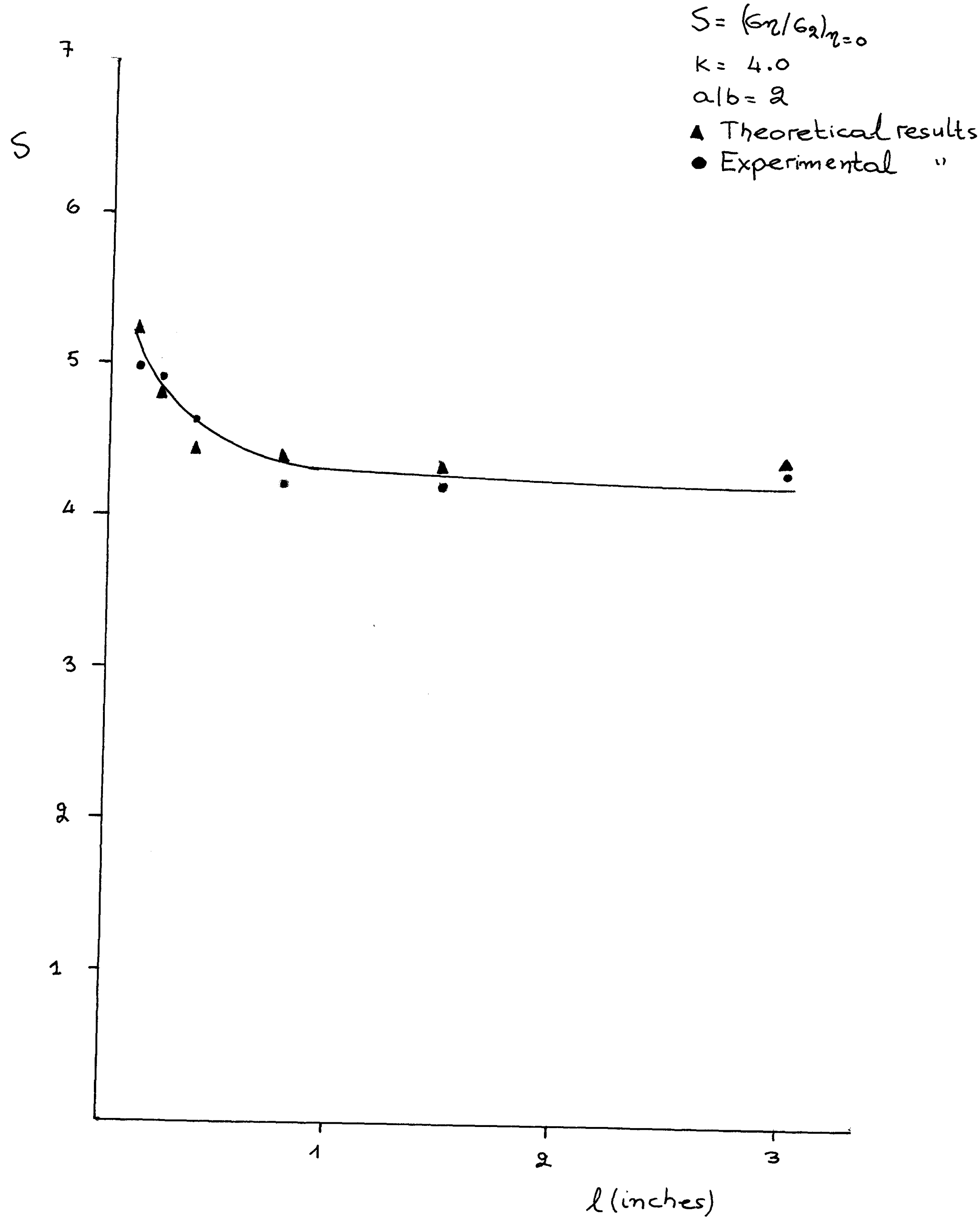
S = (σ_η/σ_2)_{η=0}
k = 4.0
a/b = 2
▲ Theoretical results
● Experimental "
S
7
6
5
4
3
2
1
1
2
3
l (inches)

GRAPH 3

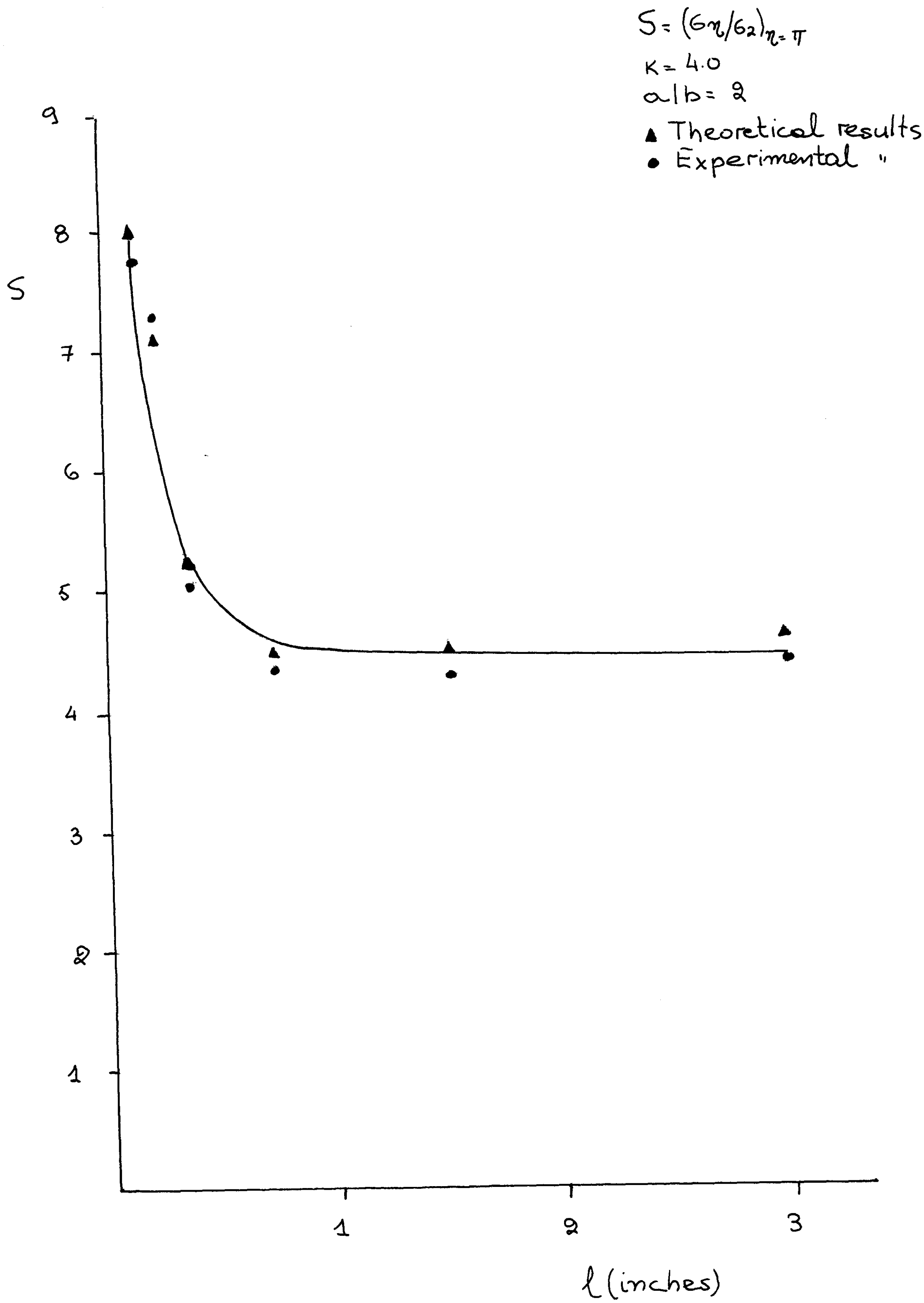
$S = (\sigma_\eta/\sigma_2)_{\eta=\pi}$
K = 4.0
a/b = 2
▲ Theoretical results
● Experimental "
S
9
8
7
6
5
4
3
2
1
1
2
3
l (inches)

GRAPH 4

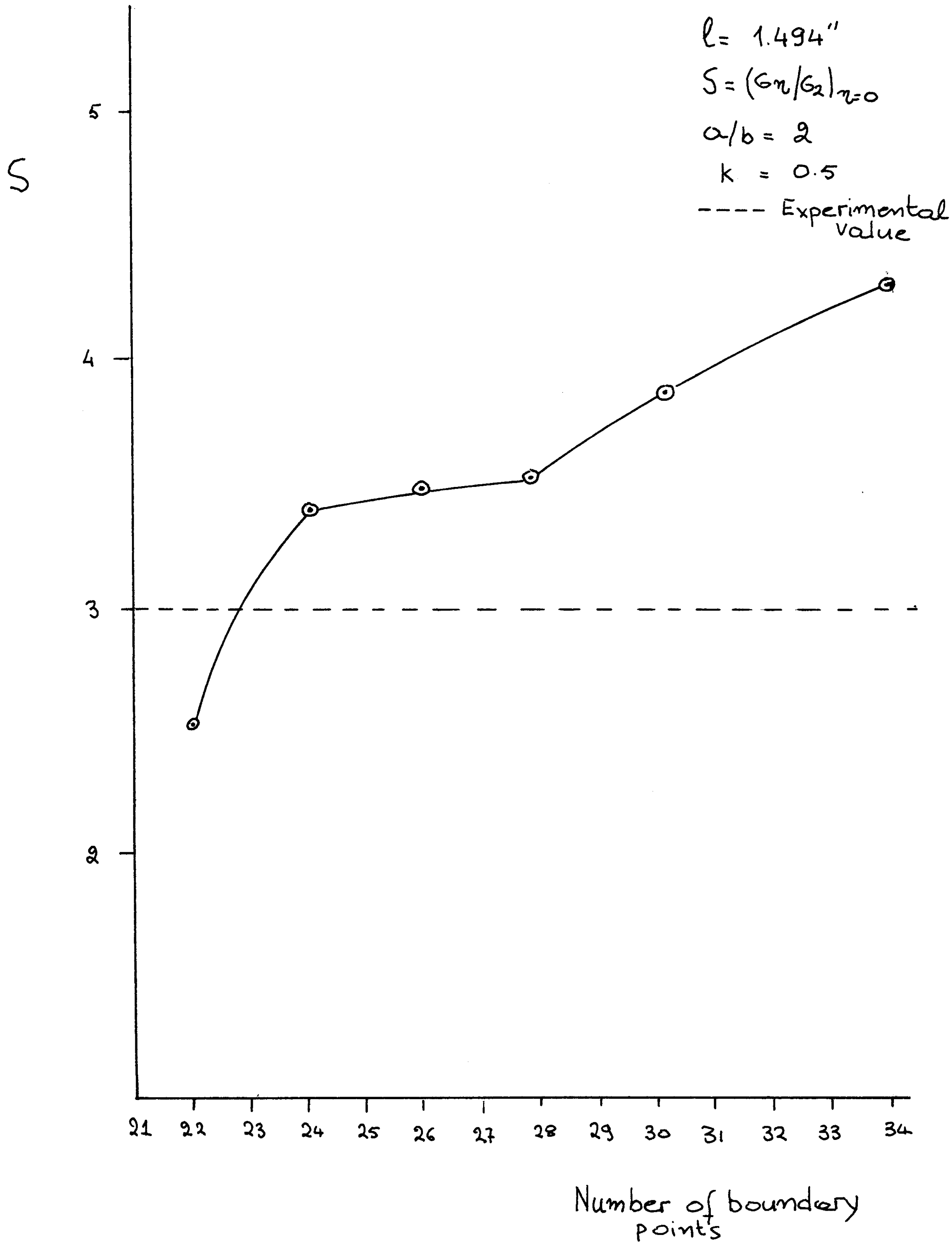

l= 1.494"
S = (Gη/G2)η=0
a/b = 2
k = 0.5
---- Experimental value
S
5
4
3
2
21 22 23 24 25 26 27 28 29 30 31 32 33 34
Number of boundary points

GRAPH 5

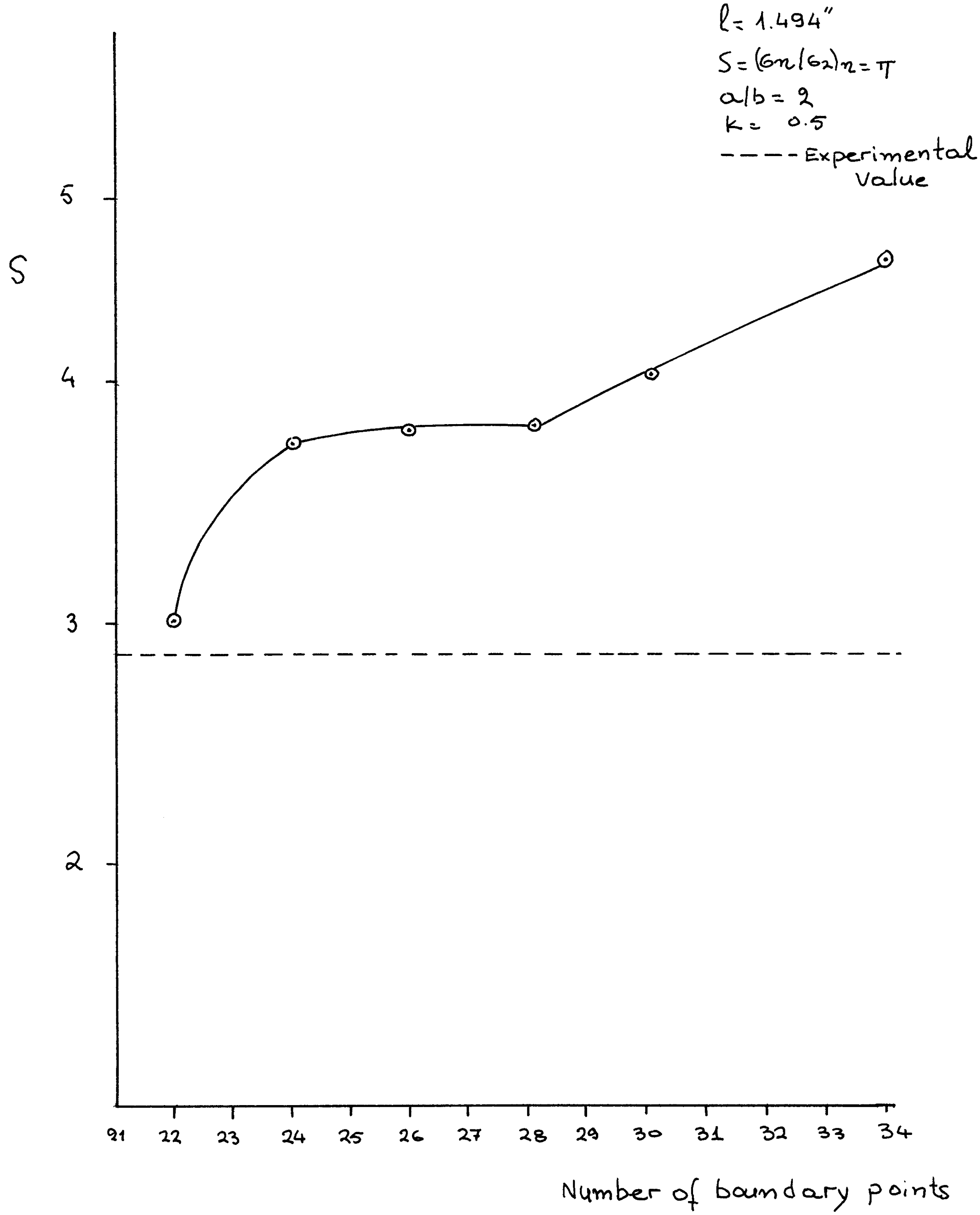
l = 1.494"
a/b = 2
k = 0.5
- - - - Experimental Value
S
5
4
3
2
21
22
23
24
25
26
27
28
29
30
31
32
33
34
Number of boundary points

GRAPH 6

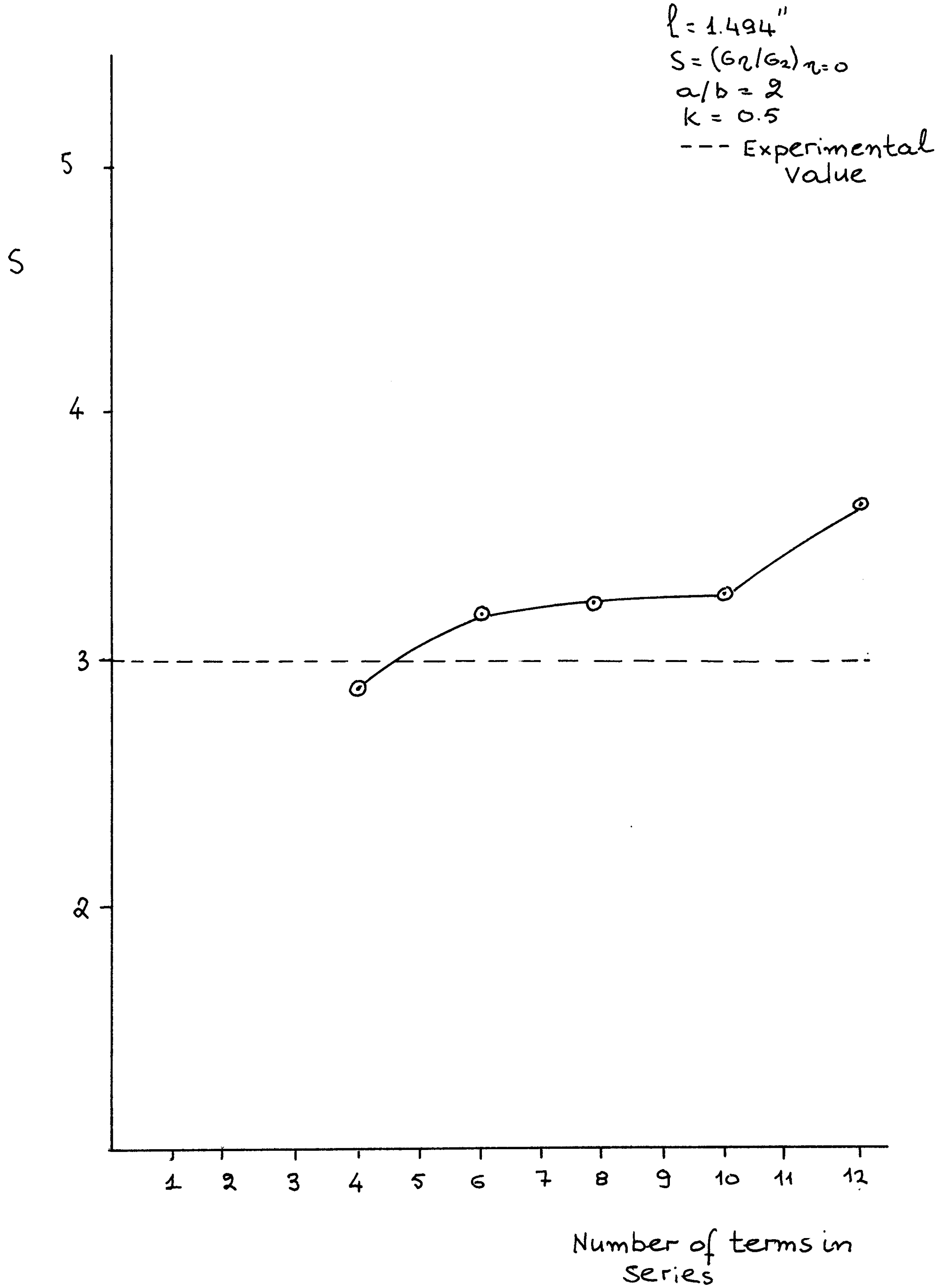
l = 1.494"
S = (Gl/G2)η=0
a/b = 2
k = 0.5
--- Experimental Value
S
5
4
3
2
1
2
3
4
5
6
7
8
9
10
11
12
Number of terms in series

GRAPH 7

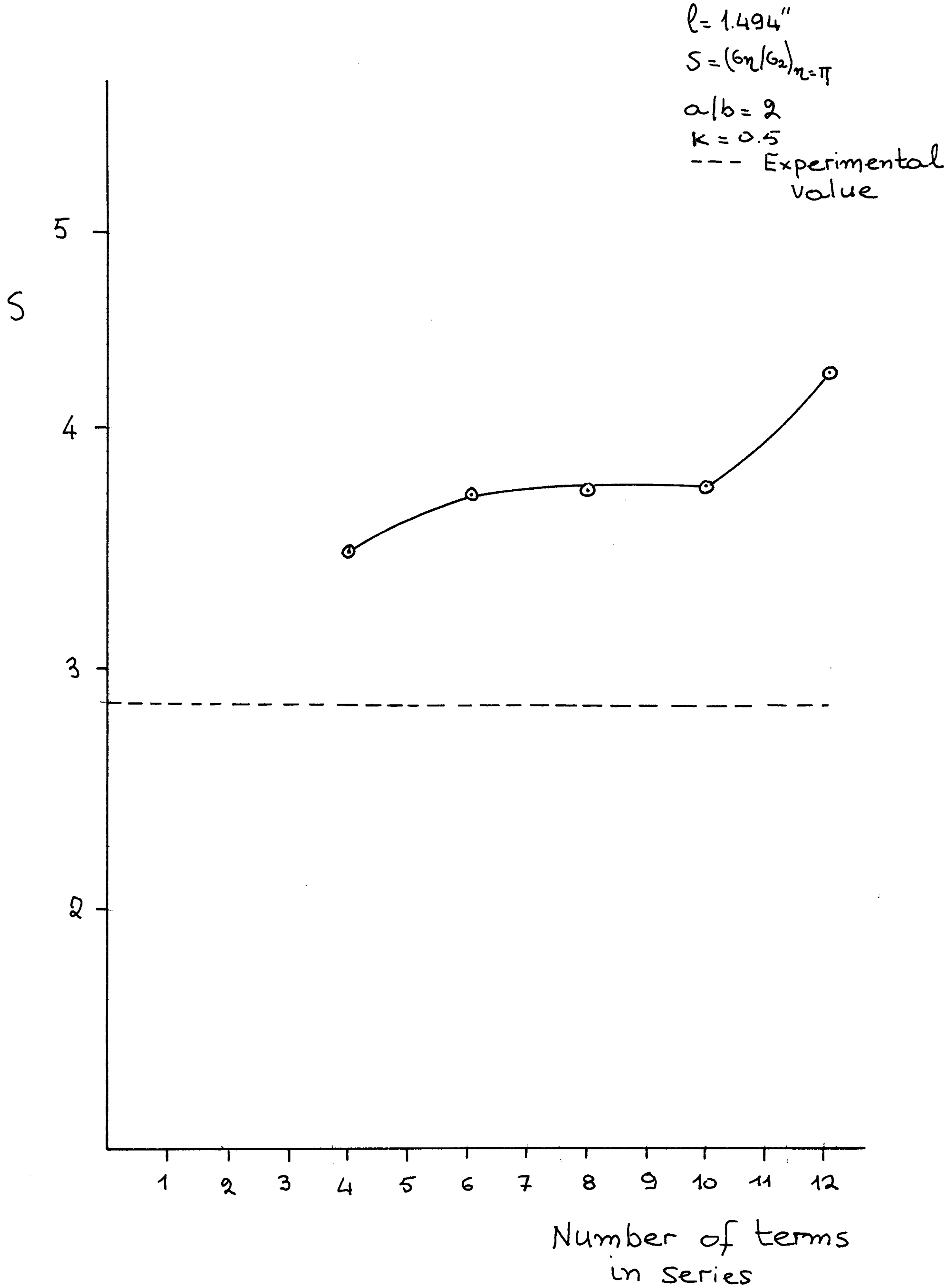

$l = 1.494''$
$S = (\sigma_\eta/\sigma_2)_{\eta=\pi}$
$a/b = 2$
$k = 0.5$
--- Experimental value
5
S
4
3
2
1
2
3
4
5
6
7
8
9
10
11
12
Number of terms in series

GRAPH 8

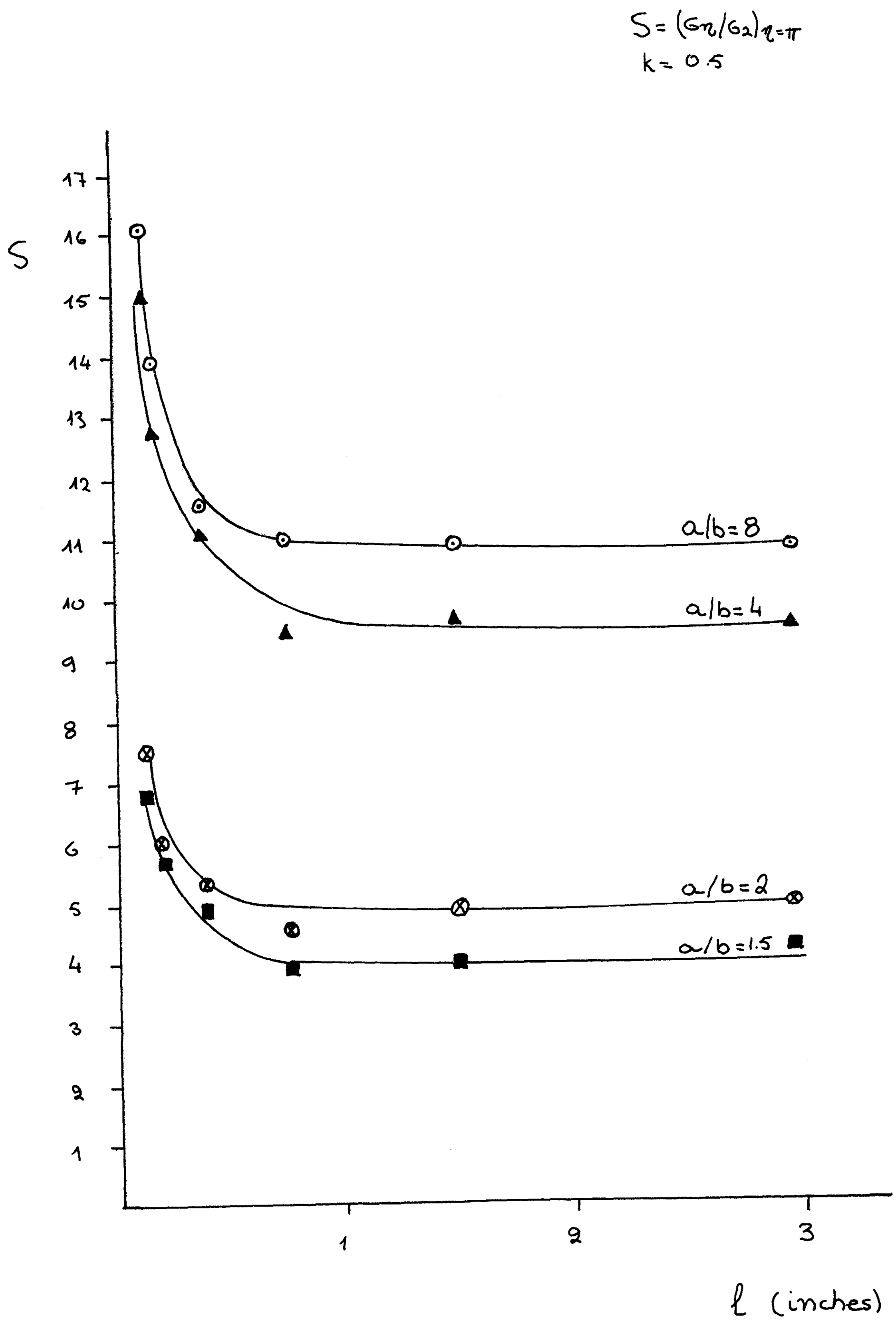

$S = (\sigma_\eta/\sigma_2)_{\eta=\pi}$
k = 0.5
S
17
16
15
14
13
12
11
10
9
8
7
6
5
4
3
2
1
a/b=8
a/b=4
a/b=2
a/b=1.5
1
2
3
ℓ (inches)

GRAPH 9

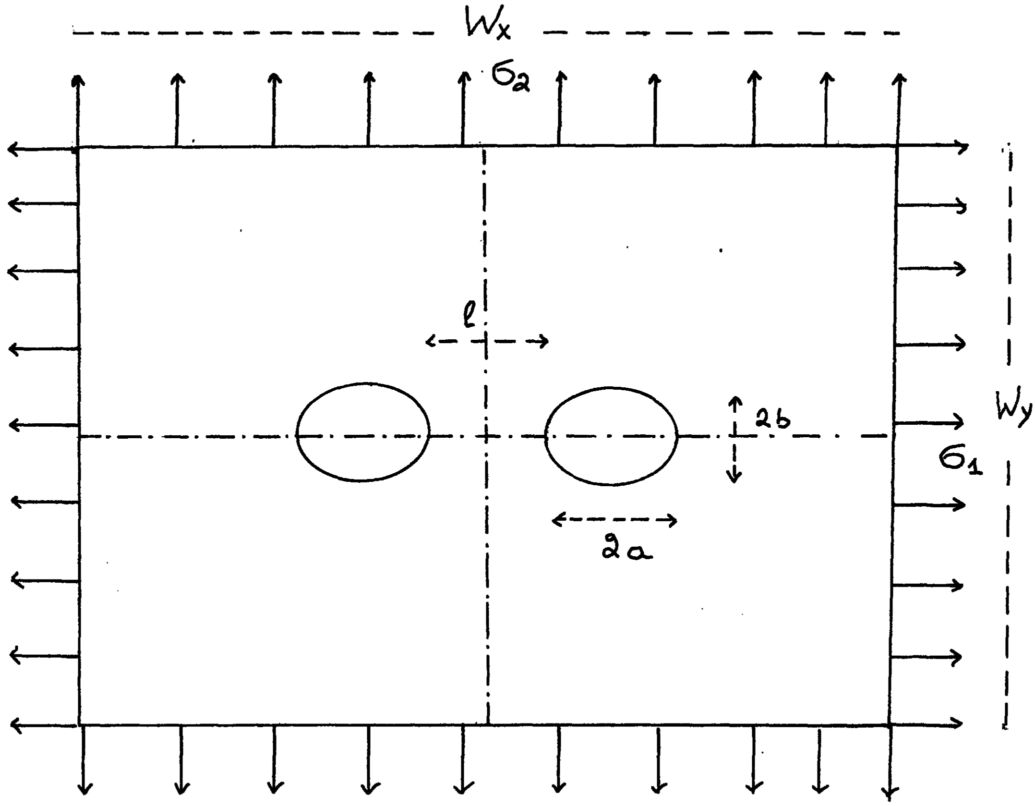

FIG. 1

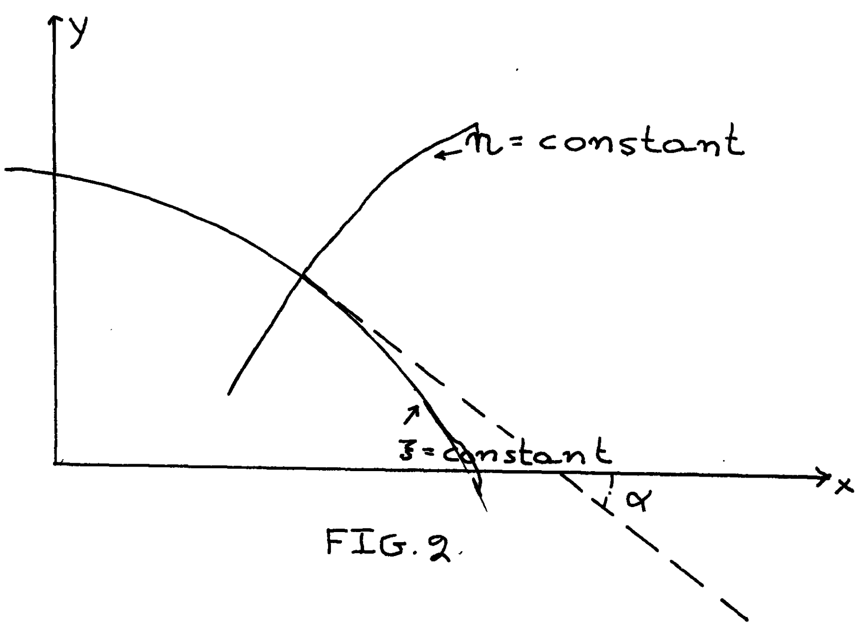

FIG. 2

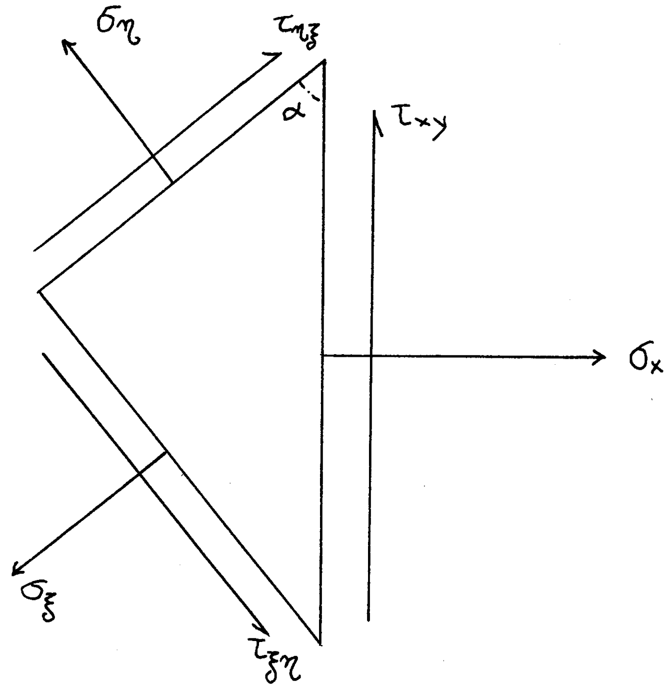

σ_η
$\tau_{\eta\xi}$
α
τ_{xy}
σ_x
σ_ξ
$\tau_{\xi\eta}$

FIG. 3

u_ξ
u_η
α
u_x
u_η
u_ξ
α
u_y

(a) FIG. 4 (b)

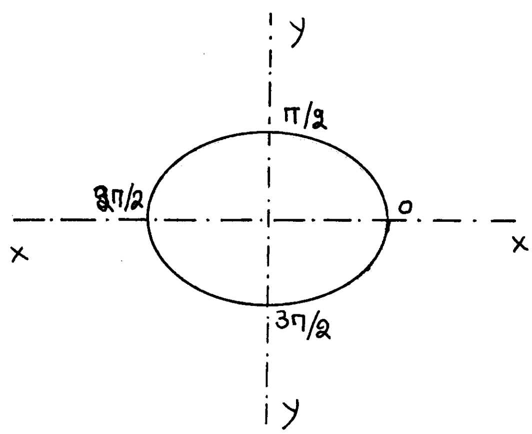

FIG. 5

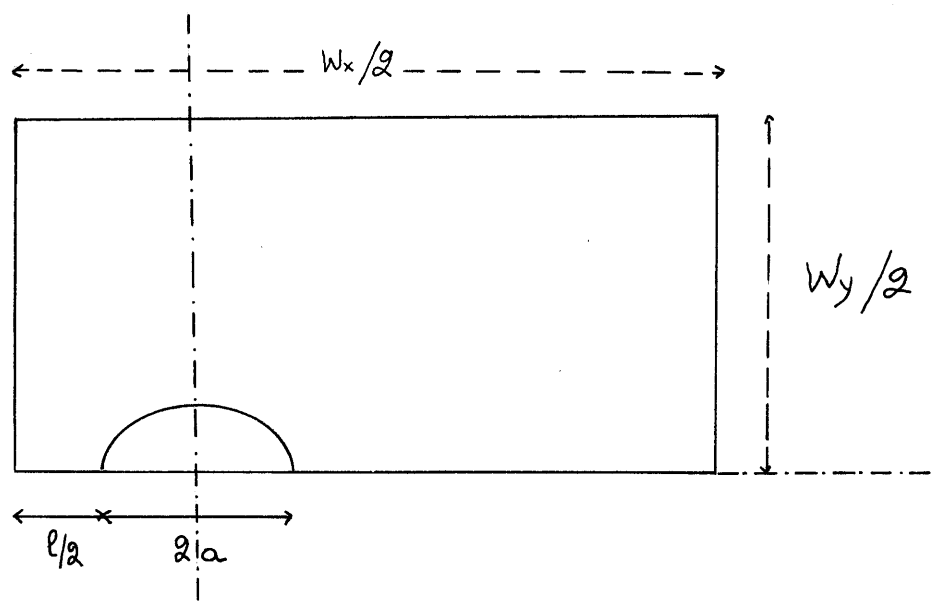

FIG. 6

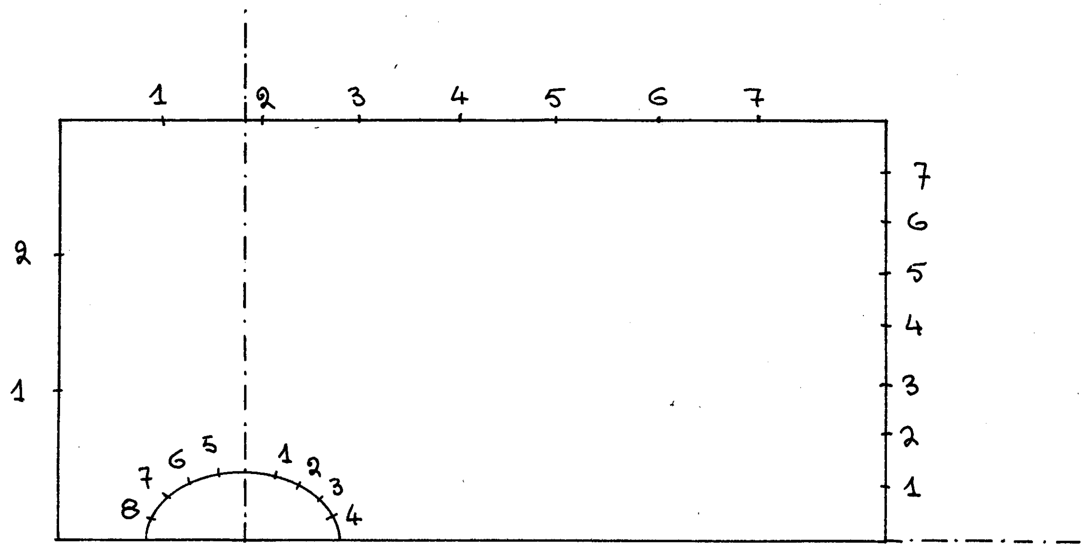

FIG. 7

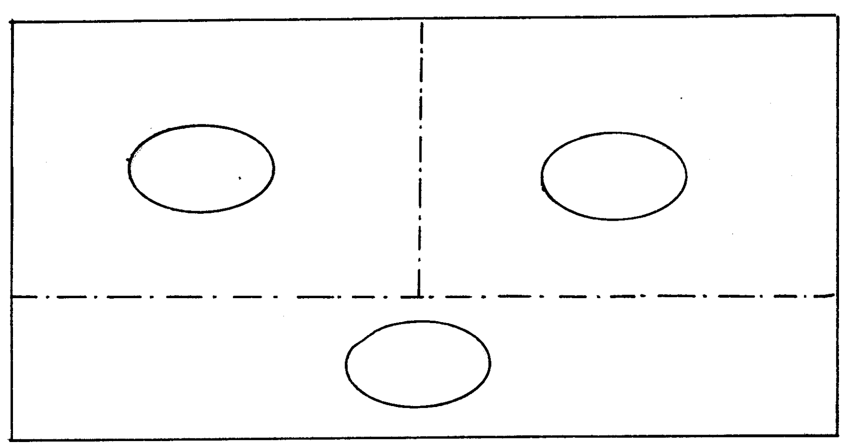

FIG. 8

NOMENCLATURE

2a = major axis of elliptical hole

2b = minor axis of elliptical hole

2c = distance between the foci of the ellipse

ξ, η = elliptical coordinates of a Cartesian point (x, y)

ξ_o = value of ξ at any point on the ellipse boundary

ℓ = separation of the elliptical holes

σ_x, σ_y = direct stresses in Cartesian coordinates

τ_{xy} = shear stress in Cartesian coordinates

σ_ξ, σ_η = direct stresses in elliptical coordinates

$\tau_{\xi\eta}$ = shear stress in elliptical coordinates

U_x, U_y = displacements in Cartesian coordinates

U_ξ, U_η = displacements in elliptical coordinates

W_x = dimension of plate in the x direction

W_y = dimension of plate in the y direction

σ_1 = uniformally distributed load applied on the edge parallel to the y axis

σ_2 = uniformally distributed load applied on the edge parallel to the x axis

K = σ_2/σ_1

Φ, ψ = stress functions

V = Poisson's ratio

E = Young's modulus (unless otherwise specified)

$\nabla^2 = \frac{\partial^2}{\partial_x^{\ 2}} + \frac{\partial^2}{\partial_y^{\ 2}}$

S = stress concentration factor = σ_η/σ_2

c_n, d_n, h_n, g_n)
)
j_n, k_n, e_n, f_n) = arbitrary constants
)
a_o, b_o)

REFERENCES

[1] T. Slot - J. P. Yalch
'Stress Analysis of Plane Perforated Structures by Point-wise Matching of Boundary Conditions,' Nuclear Engineering and Design, Vol. 14, No. 2, pp. 63-176, Aug. 1966.

[2] N. Jones - D. Hozos
"A Study of the Stresses Around Elliptical Holes in Flat Plates', ASME, Vol. 93, Aug. 1970.

[3] A. Timpe
'Die Airysche Funktion für den Ellipsenspring', Mathematisch Zeitschrift, Vol. 17, p. 189, 1923.

[4] J. W. Hansberry - N. Jones
'Elastic Stresses due to Axial Loads on a Nozzle which Intersects a Cylindrical Shell', ASME, Vol. 1, pp. 129-154, 1973.

[5] E. G. Coker - L.N.G. Filon
'A Treatise on Photo-Elasticity' revised by H. T. Jessop, Cambridge University Press, 1957.

[6] J. E. Goldberg - K.N. Jabbour
'Stresses and Displacements in Perforated Plates', Nuclear Structural Engineering, Vol. 2, p. 360, 1965.

[7] N. Jones
'Comments on Statics and Dynamics of Elastic Sheels with Cutouts - A Review by J. Pattaba-rinaman, V. Raamamurti, D. V. Reddy', Journal of Ship Research, Vol. 19, March 1975, p. 62.

[8] System/360 Scientific Subroutine Package (360A-CM-03X), Version III.

[9] A. J. Durelli, V. J. Parks, H. C. Feng
'Stresses Around an Elliptical Hole in a Finite Plate Subjected to Axial Loading', Journal of Applied Mechanics, ASME, Series E, Vol. 88, No. 1, 192-195, 1966.

[10] A. H. Cotrell
'The Mechanical Properties of Matter', London 1964, pp. 108-115.

ACKNOWLEDGEMENTS

The author would like to thank Professor Norman Jones from whom most of the theory used in this thesis is drawn, for his continuous guidance and encouragement and also his extreme interest as a thesis supervisor.

TABLE OF CONTENTS

Page